# Acousto-Ultrasonic Evaluation of Cyclic Fatigue of Spot Welded Structures

by

Brian M. Gero

Thesis submitted to the Faculty of the
Virginia Polytechnic Institute and State University
in partial fulfillment of the requirements for the degree of

MASTER OF SCIENCE
IN
ENGINEERING MECHACNICS

APPROVED:

_____
J. C. Duke, Jr., Chair

_____ _____
N. E. Dowling E. G. Henneke

August 28, 1997
Blacksburg, Virginia

**Keywords:** NDE, Acousto-Ultrasonic, Fatigue, Spot weld, Ultrasonic

# Acousto-Ultrasonic Evaluation of Cyclic Fatigue of Spot Welded Structures

By

Brian M. Gero

Dr. John C. Duke, Jr., Chairman
Engineering Mechanics

## ABSTRACT

An acousto-ultrasonic approach is used to explored the damage development in tensile shear spot welds during fatigue loading. There is reasonable data to support the hypothesis that a decrease in an AU signal is indicative of the presence of an internal crack and could be used for monitoring and evaluation purposes.

## Acknowledgements

I would like to thank Dr. John C. Duke, Jr. for his guidance, support, and understanding as my committee chair. Dr. Norman Dowling has been an invaluable asset to this project and to my success. Dr. Dowling, I extend my deepest gratitude. I wish to thank Yuting Rui and FORD motor company for their funding and support. I would also like to thank Dr. E. G. Henneke for taking the time to join my committee on such short notice and for his advice on many occasions. I would like to recognize and thank John “Andy” Newman for his countless hours behind the controls of MTS machines and his effort to keep things light-hearted and for his encouragement. To my fiancée, Jennifer, thanks for your encouragement and dedication. To the many others who have listened to my complaining and still speak to me, thank you all.

## Table of Contents

## List of Figures

## List of Tables

# 1. Introduction

## *1.1 Motivation*

Spot welds are crucial to the automotive industry. They make up a large percentage of the joints that hold an automobile together. In fact, "the typical car body contains about 5000 spot welds joining a mixture of sheet metal material types and thicknesses." [(1)] One of the major concerns in the spot weld industry is fatigue. The only visible sign of spot weld degradation due to fatigue is a crack at the surface of the weld. Unfortunately, the crack does not begin at the exterior surface. Therefore, it would be beneficial to manufacturers if they were able to detect a crack in the spot welded member, determine the severity of the damage, and the remaining serviceability of the spot weld, before it reached the exterior surface and proceeded to rupture. Until recently, with the advent of non-destructive evaluation methods, this was not a viable possibility. However, with technological advances and new methods, the means and equipment exist for analyzing spot welds for damage in a non-destructive manner.

## *1.2 Project Details*

This research has been sponsored by Ford Motor Company with two areas of focus. One task involves life prediction of spot-weld fatigue. This research is done to provide insight into the mechanics of spot-weld fatigue in other geometries as applicable to the automotive industry. The results of this research

can be found in the master's thesis of John Newman.[2] This paper will focus on the other task of the research: determining an effective means by which to detect fatigue cracks and evaluate the remaining serviceability of spot-welded structures in a nondestructive manner.

Ford has provided specimens of two different materials, 950X steel and 1010 steel. The specimens are general coupon specimens as seen in Figure 1.1. The weld in question is that which joins the two sheets of metal. The specimens were received in two batches. The first batch were labeled in the form L1-1XX and L9-1XX, where the first two characters refers to the type of specimen and the material. More specifically, L refers to lap-joint specimens, 1 refers to 1010 steel, 9 refers to 950X steel, and the 1XX is the specimen number, beginning with 100. The second batch of specimens was labeled in the same manner with the specimen numbers beginning with 200.

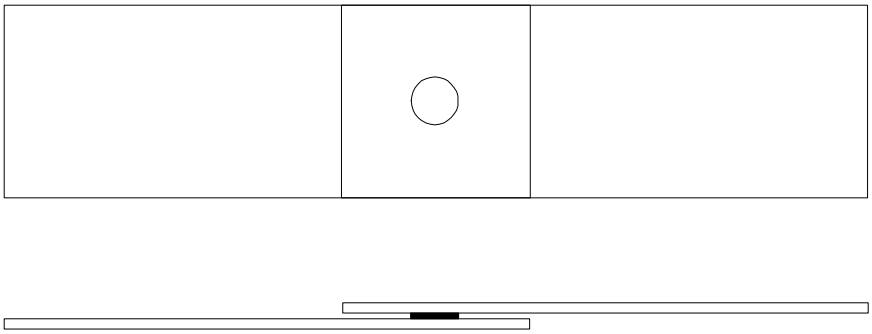

**Figure 1.1 Top and side sketch of tensile shear spot weld (lap shear) specimen.**

The coupons represent the general form (shape/description) of the spot weld. The researchers realize that not all spot welds are found in this geometry, and that these specimens are only representative of the loading scenarios.

## *1.3 Literature Review*

Spot welding is the most common method of joining two strips of metal and has been studied for many years. In the industry's never-ending goal to reduce weight and increase performance, the spot welded joint has seen many changes. Manufacturers are using thinner, higher-strength steels for weight reduction. While these metals may exhibit higher strength properties under static conditions, the effects of the higher strength steels on high-cycle fatigue lives are negligible.[2,16] This has drawn attention to the behavior of spot welds under fatigue loading. It would not be unreasonable to assume that spot welds with few or no flaws or defects would exhibit higher fatigue lives than spot welds found to have defects.

### 1.3.1 NDE Spot Weld Work

In order to determine the quality of the weld, different methods have been applied. The most common method of monitoring spot weld quality is the teardown method combined with visual inspection. Mansour shows that ultrasonics is a viable means for spot weld quality inspection[1]. His research focuses on comparing the ultrasonic method to the teardown method for the

classifications of weld quality. He finds that by using the ultrasonic pulse-echo method, it is possible to correctly classify over 99% of the welds he sampled.

Expanding on the use of ultrasonics to monitor and classify inadequate welds, Rokhlin, Meng, and Adler developed a method for *in-process* inspection of spot welds[(2)]. The underlying premise of their research was to compare two different methods of ultrasonically inspecting spot welds while they were being formed. The two methods involved were ultrasonic Lamb waves and through-longitudinal waves transmitted via transducers mounted in the welding electrodes. In their research, Rokhlin, Meng, and Adler showed how the ultrasonic signal was affected by the temperature changes in the weld during processing, allowing the monitoring of the phase changes in the weld as well as the monitoring of the cooling phase. They also showed that the ultrasonic signal is transmitted from one sheet to the other via the weld, as well as directly from one face of the weld to the other.[(3)]

### 1.3.2 Previous Work Using Ultrasonics to Test Fatigue of Spot Welds

Ultrasound is not a new technique to the spot weld industry, for previously it has been used in different capacities. Most of the non-destructive techniques have been used to evaluate the actual quality of the weld itself (due to processing), as opposed to evaluation of fatigue properties as described above.

However, there have been studies done on the development of fatigue cracks in spot welds using a method termed *electric-potential-drop*.[4,15] This method is similar to a non-destructive evaluation method in that it uses the change in the voltage between two electrodes to define either crack growth or plasticity effects. The plasticity effects are interpreted using a correction factor. The presence and propagation were validated by sectioning and by freezing with liquid nitrogen, breaking the specimens, then measurement of the crack. Some important conclusions were drawn from these experiments. Cooper and Smith found that the crack growth, with respect to load cycles, through the thickness of the plate, was predominantly linear for spot-welds whose crack penetration fell within the range of 0.2mm and 1.12 mm.[15] Swellam, Kurath, and Lawrence found that there was little correlation between the potential difference and crack depth during stage I [4]. They also suggested that stage I accounts for more than 40% of the total life of their galvanized low carbon steel. However, there did exist an agreement during stage II, where the potential difference readings were caused by the propagation of a major crack.

It is the purpose of these experiments to identify the onset of a crack, monitor it during its initiation and development through the sheet metal, and evaluate the remaining serviceability of the spot weld coupon.

### 1.3.3 ***Acousto-Ultrasound***

#### 1.3.3.1 Methodology and Background

Nondestructive evaluation is a rapidly growing industry and is becoming a critical aspect of many businesses. Its applications are growing almost as rapidly, and with new applications, there must be techniques with which to evaluate these situations or applications. In the late 1970's Alex Vary introduced acousto-ultrasound (AU). It is a technique which combines two common and respected forms of non-destructive testing: acoustic emission (AE) and ultrasound.[5,20] Conventional acoustic emission methods are based on the stress waves produced internally by defects, e.g. crack propagation or plastic deformation. Acousto-ultrasonics, however, uses an external ultrasound source to excite stress waves and acoustic emission methods to detect and analyze the propagated signal.[6]

It is important to recognize the difference between the AU method and pitch-catch ultrasonics. In pitch-catch ultrasonics, the path of the wave is traceable. In acousto-ultrasonics, however, the introduction of the pulse into the specimen yields mixed modes of propagation whose paths are difficult to trace throughout the specimen.[14] These mixed modes of propagation ultimately result in the disturbance of the surface at the point of detection.

This approach is based on how well the stress wave energy can propagate through a material and how it interacts with the microstructure. The underlying

principle of AU is that if the stress wave energy is not efficiently distributed through the material, then the applied load is more likely to promote cracking in the inefficient regions of the material than in regions with more efficient energy transmission. Therefore, if the stress waves are efficiently transmitted, more efficient strain energy transfer will occur, which is associated with an increased mechanical strength.[5,7]

Another basis for this approach is the assessment of the specimen as a whole while it is in its relaxed state. In normal AE testing, it is necessary to apply a load to the specimen in order for it to generate the necessary stress waves for detection. In AU, the stress waves are stimulated with the ultrasound signal. Also, often in AE or ultrasound, the results of the evaluation are specific to the area of the specimen where the flaw exists. With AU, its concentration is on assessing the serviceability of the specimen, rather than characterizing the flaw.

#### 1.3.3.2 Signal Analysis

The analysis of the waveform is primarily done using acoustic emission (AE) technology. One method for quantifying the waveform detected by the receiving (or AE) transducer is using what is referred to as the *stress wave factor* (SWF). The SWF is a measure of the stress wave energy that propagates through the specimen. This SWF is used to quantify the AU signal in terms of the material's mechanical properties. In general, if the SWF is high, less attenuation has occurred and the material has efficiently transmitted the stress wave energy.

Often, better stress distribution, or stress wave energy transfer, relates to an increase in strength and fracture resistance. The SWF can be defined in more than one way, depending on the application, specimen, and material characteristic being explored. Some common ways come directly from AE methods: ringdown count, peak voltage, and energy.[5,8]

The ringdown count is the product of the repetition rate of the ultrasonic pulser, the reset time in the receiver, and the count, the number of oscillations which exceed a preset threshold voltage: $E_{SWF}$ = (R) (T) (C). The peak voltage method of quantifying the SWF relies on the peak value of an energy envelope created from the waveform. The energy method is similar to the peak voltage in that the energy envelope waveform is subjected to a spectral analysis and the SWF is assigned the peak value of the spectrum.[5,8]

Although ringdown counting is the most common method for measuring an acoustic emission signal,[12] the difficulty with this method is that the AU signal changes as the defect in the material grows. Therefore, it becomes much more difficult to make an accurate mathematical model of the signal and consequently more difficult to directly relate the ringdown counts to the energy of the signal.

Sundaresan and Henneke discuss other methods for quantifying and measuring the content of the energy in an AU signal. One particular method involves a measurement of the RMS voltage. There are studies which show the correlation

between the frequency spectrum of the waveform and the moments of the AU signal as described in equation 1.3.1:

$$M_r = \int_0^\infty S(f) f^r df \ , \qquad (1.3.1)$$

where $M_r$ is the zeroth moment, S(f) is the power spectral density, and f is the frequency. An integration of the Fast Fourier Transform of the frequency spectrum of the AU signal of these moments yields a correlation between the zeroth moment and the level of damage to the material. It is also shown that the RMS voltage measurement was equivalent to the zeroth moment of the AU signal.[13,22] This indicates that by measuring the RMS voltage, it is an assessment of the amount of damage to a material.

#### 1.3.3.3 Application Constraints

One challenge we faced was the monitoring of the spot weld during fatigue cycling. We attempted five different NDE methods with little success: magnetic particle inspection, liquid penetrant, eddy current, the Scanning Acoustic Microscope (SAM), and C-scanning. Specifically, magnetic particle inspection was not an adequate candidate as its equipment was too bulky to fit onto the specimen while it was mounted in the machine. Liquid penetrant was not able to detect the cracks early enough. Further, eddy current data were difficult to interpret, nor could we determine whether or not the data were useful. Thus, we chose acousto-ultrasonics. With the AU equipment, the transducers are small

enough to be mounted on the specimen without causing interference with the MTS machine.

Another constraint affecting our method of choice was the geometry and nature of the weld. Some methods require a smooth surface for inspection. For example, to employ the eddy current method, the surface must be relatively smooth and an appropriate probe must be used. After consulting with Zetec, a leading manufacturer of eddy current probes, it was determined that a cylindrical probe would be best suited for the spot weld. The probe resembled a ¼" thick washer with the coil wrapped between the inner diameter and outer diameter. Upon testing, however, it did not perform as anticipated. It was difficult to interpret the data received from the probe and the probe was prone to lift-off effects and offered little hope for effectiveness. Therefore, the eddy current method was abandoned.

Different ultrasonic scanning methods were also considered as methods of evaluation of the spot weld. Both the Scanning Acoustic Microscope (SAM) and C-scan were evaluated. Both involved submerging the specimen in a water bath and performing an echo ultrasound on the specimen. Although water is one of the best couplants available, the SAM required a very smooth surface and was somewhat limited on depth penetration when a detailed image is required. To evaluate each specimen, the weld must be ground and polished to provide a smooth surface for the scan. The SAM was also found to be an unacceptable method for this particular use because it is not portable.

C-scanning refers to a method of scanning which builds an image of the specimen from a gated signal. The machine jogs forward at a preset distance while the transducer is moving back and forth across the sample. We found this method to be very tedious, time consuming, and not as effective as the AU for monitoring damage development.

#### 1.3.3.4 Monitoring Degradation

During fatigue cycling, the spot weld is constantly being weakened. It has been shown that crack propagation begins early, but that most of the damage and propagation occur well after the onset of the crack initiation. It was postulated that as the crack initiates and propagates, the AU signal will begin to decrease. As the crack grows, the crack surface area will increase, causing interference in the signal being transmitted to the receiving transducer.

#### 1.3.3.5 Mode of Degradation

The premise underlying our method of choice is that the crack propagates in a plane perpendicular to the surface of the weld until it gets to the surface at an angle of approximately 60° [(4)], as shown in Figure 1.3.1. As it appears at the surface along the interface between the weld and the base metal, it proceeds to propagate out into the base metal towards the edge of the specimen, in the form of an eyebrow crack, until the specimen ruptures (defined to be 50% of the circumference of the weld).

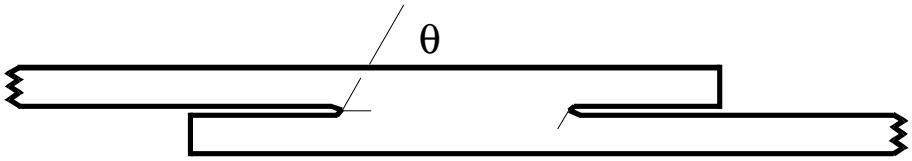


**Figure 1.3.1 Sketch showing angle of crack propagation, θ.[(2)]**

A basic mechanics analysis reveals that the primary forces acting on an element of the weld, as shown in Figure 1.3.2, are shear and normal forces perpendicular to the loading. This indicates that at the failure point C or D in Figure 2.4.1, the stress intensities are at maximums for failure modes I and II. A more detailed analysis can be found in John Newman's thesis.[(2)]

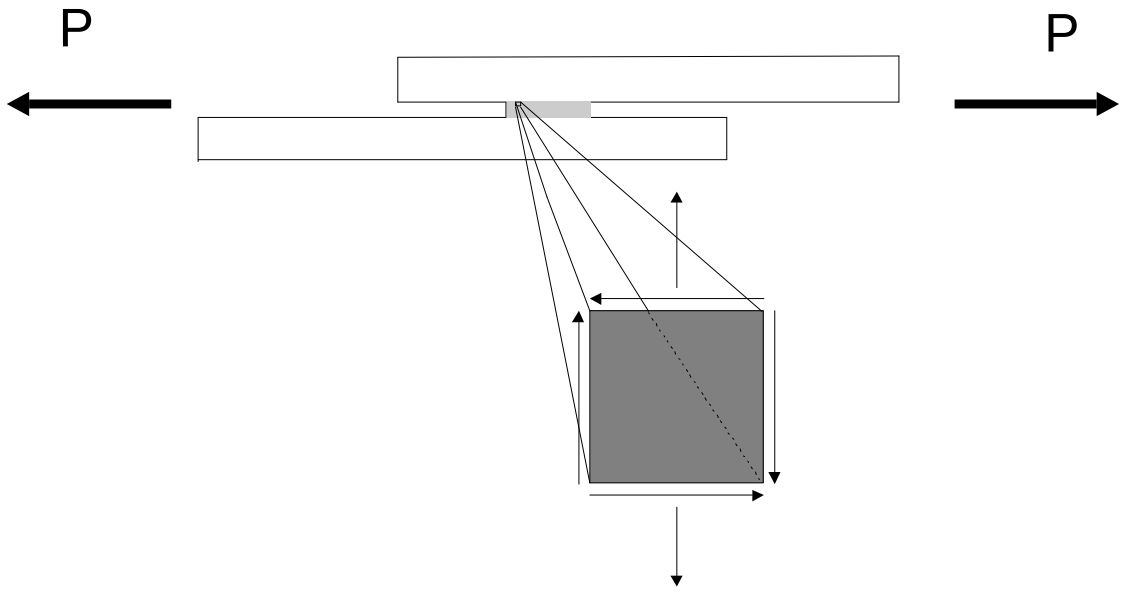


**Figure 1.3.2 Static description of an element of the weld under loading (P).**

The ultrasonic signal is transmitted from one face of the sample to the other through the weld, as seen in Figure 1.3.3. While most of the wave in region I enters the weld region, section III, the part of the wave which encounters the slit at L1 is reflected back into region I and part is diffracted into region I'. From

region III, the wave is transmitted and diffracted into regions II and II'.[3] As a crack is formed and begins to propagate, the pulsed signal will intersect the crack and be dispersed throughout the material lessening the signal strength detected by the acoustic emission transducer. In order to increase the ultrasonic energy propagation in the plane of the plate and thereby increase the interaction with cracks growing near the weld, an angled beam transducer was used as the ultrasonic source. A similar transducer was used as the detector.

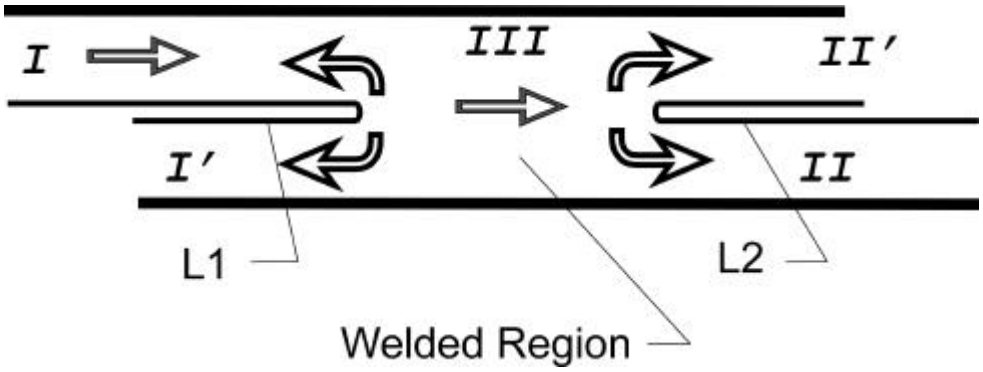


**Figure 1.3.3 Description of ultrasonic signal transmission through weld.[3]**

### *1.3.4 Welding Process and Fatigue*

#### 1.3.4.1 Welding Process

The electrical resistant spot welding process involves joining two pieces of sheet metal through the use of electrical current. The pieces of sheet metal are clamped together and a current is passed through two copper electrodes placed on either side of the sheets. As the current passes through the sheets, the resistance to the current generates the heat which melts the metal while pressure is applied by the electrodes.[18,19] Some factors which affect the performance and quality of the spot weld are: electrical current, diameter of weld nugget (diameter of electrode), electrode force, hold cycles, and weld cycles. Studies have been conducted on the diameter of the weld nugget in relationship to the thickness of the base metal as it affects the fatigue life.[18] Other studies have been done on the high temperature effects from the welding on the base metal around the weld nugget, known as the heat-affected zone (HAZ).

#### 1.3.4.2 Fatigue

There are two primary schools of thought on how the fatigue of a spot weld should be modeled. Cooper and Smith support the theory that the spot weld is a sharp notch and fatigue of the spot weld consists of two stages – initiation and propagation. [15,20] The other school of thought is supported by F. V. Lawrence and others who believe the fatigue of spot welds is a three stage process. Stage I is devoted to initiating a crack of an arbitrarily small length (~0.25mm). Stage II

is crack propagation through the HAZ to the exterior surface of the base metal as shown in Figure 1.3.3; and in Stage III the crack propagates around the circumference of the weld then out into the base metal perpendicular to the loading until it ruptures.[18,4] It has been suggested that as much as 50% of the fatigue life can be spent developing Stage I.

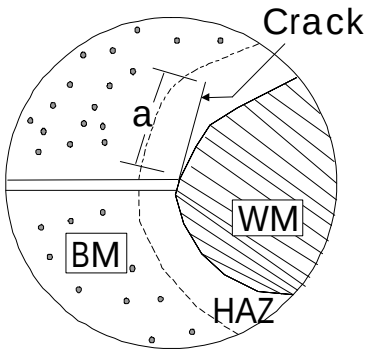


**Figure 1.3.3 Crack initiation and propagation in the HAZ of Stage II.**[after 17]

Figure 1.3.4 may help to visualize the formation and propagation of a crack in a tensile shear spot weld. In all three diagrams, the sectioned view of the weld is shown above a top view. Figure 1.3.3 (A) shows the crack in its early stage where it is internal. (B) shows the crack as it has propagated through the thickness and is prepared to break through the surface causing a dimple-like feature on the surface. (C) shows the crack through the surface and propagating along the circumference of the weld nugget in an *eyebrow* shape.

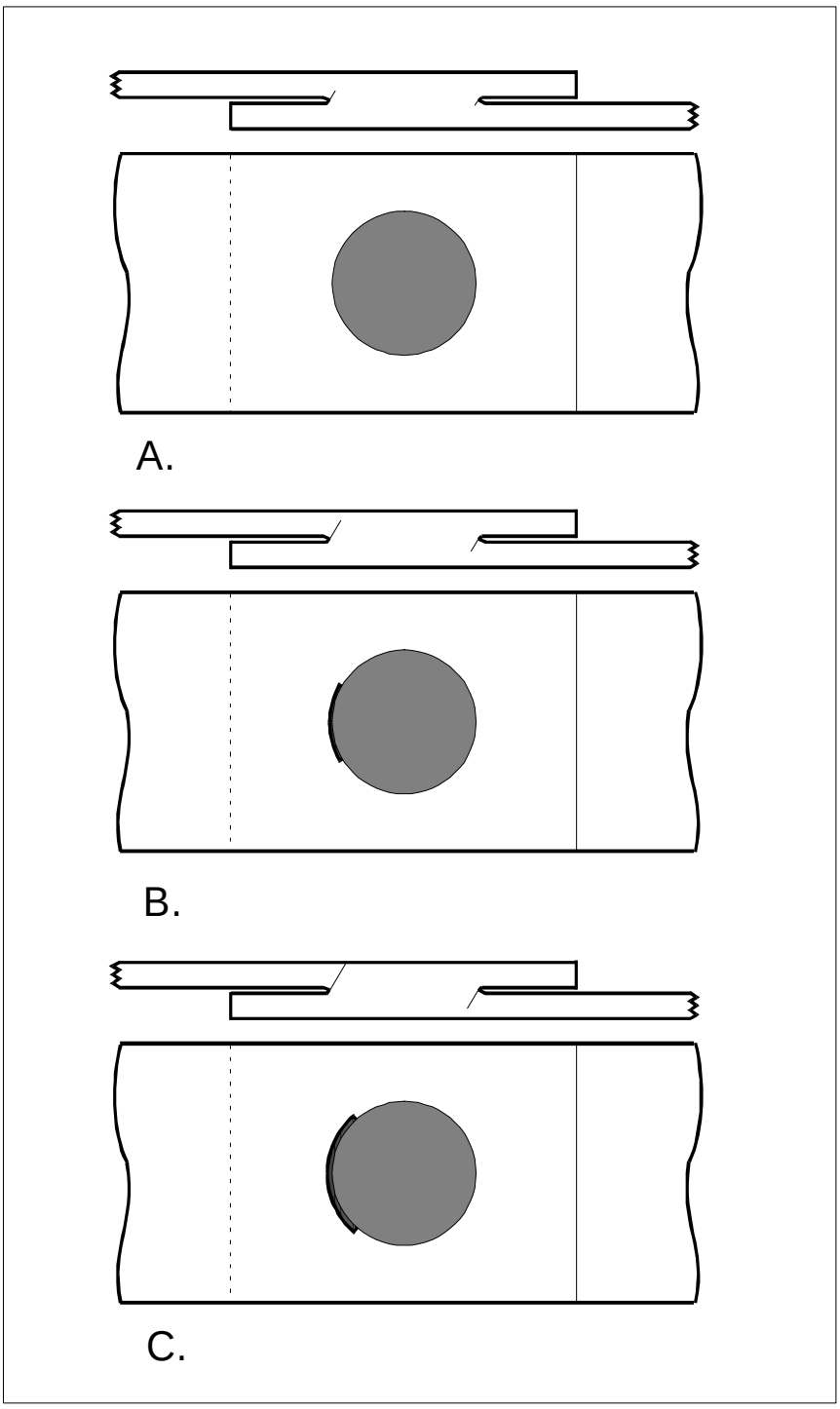


**Figure 1.3.4 Depiction of crack formation: (A) early stages, (B) propagating through the thickness to exterior surface, and (C) propagating around the circumference of the weld. Shown are a side view and top view of a tensile shear spot weld.**

## 2. Experimental Methods

This section will describe the methods used to perform the fatigue testing, the acquisition of acousto-ultrasound data, radiography, and the metallography of the specimens.

### *2.1 Fatigue Testing*

The fatigue testing was performed on both 10 kip and 20 kip MTS servo-hydraulic testing machines. The 10 kip machine was equipped with a 458.20 controller, while the 20 kip machine was controlled by TESTAR, a software package specifically designed for running fatigue tests. All tests were performed using a sinusoidal waveform operating primarily at 10 Hz in air at room temperature. The specimens were mounted in the grips 0.75” from both ends. In order to provide symmetry and to prevent a moment being applied at the weld, one inch long shims, with the same thickness as the sheet metal, were glued at either end of the specimen as shown in Figure 2.1.1. All of the specimens were made by FORD to be as close to identical as possible.

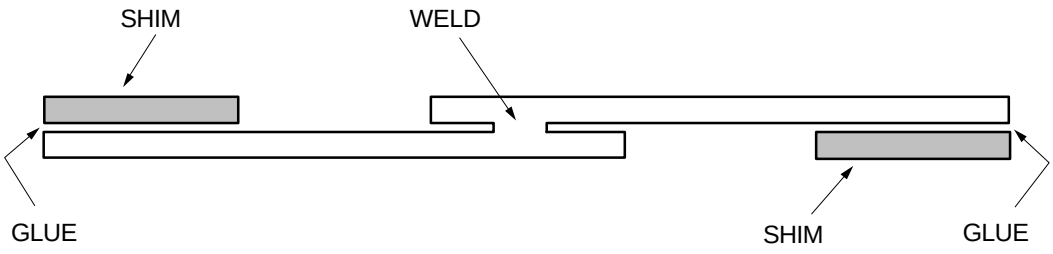


**Figure 2.1.1 Sketch of typical lap joint specimen with shim attached.[2]**

Tensile tests were used to determine the ultimate strengths of the spot-welds. Those results were then used as a basis for determining appropriate load levels for fatigue testing. Complete tables of the fatigue results can be found in John Newman's thesis[2]. An R-ratio of 0.1 was used for all the testing related to AU inspection. The fatigue life cycles to failure were used as a basis for determining percentages of life for stopping the AU inspection and performing radiography and/or sectioning and polishing. For example, we cycled the mild steel (1010) to approximately 85% of the life and then made adjustments between 85% and 5% to attempt to determine when the crack initiated and its propagation.

The load levels for both steels were chosen to maximize a reasonable amount of data taken in a reasonable time frame. The 1150 pound and 900 pound load levels for the mild steel had fatigue lives of approximately 9500 cycles and 25000 cycles respectively.

### *2.2 Acousto-Ultrasound Acquisition*

We used 60° angle beam transducers both for sending the signal and for the acoustic emission "listening" by the receiver. It was necessary to use a preamplifier in between the receiving transducer and the receiver unit to amplify the signal an additional 40 decibels, over and above the existing 20 dB gain present in the receiver. The sending and receiving transducers were placed 1"

apart, .5” on either side of the weld, on the opposite surfaces of steel. As the signal was received, it was gated by the receiver in order to isolate the part of the signal that comes directly from the sending transducer. The settings for the pulser/receiver were as follows:

| | |
|---|---|
| gain: | 20 dB |
| rep rate: | 1000 Hz |
| receiver attenuation: | 0. |

The signal was then output to a Hewlett Packard model 3400B RMS voltmeter set to a range of 0 - 0.1 volt. The RMS voltmeter estimated the average amount of energy in the detected signal. Figure 2.2 is a schematic of the setup. The signal from the voltmeter was recorded using a Gould model TA240 electronic strip chart with the following settings:

Range: 1 volt full scale,
Chart Rate: 1 mm/sec,
DC signal.

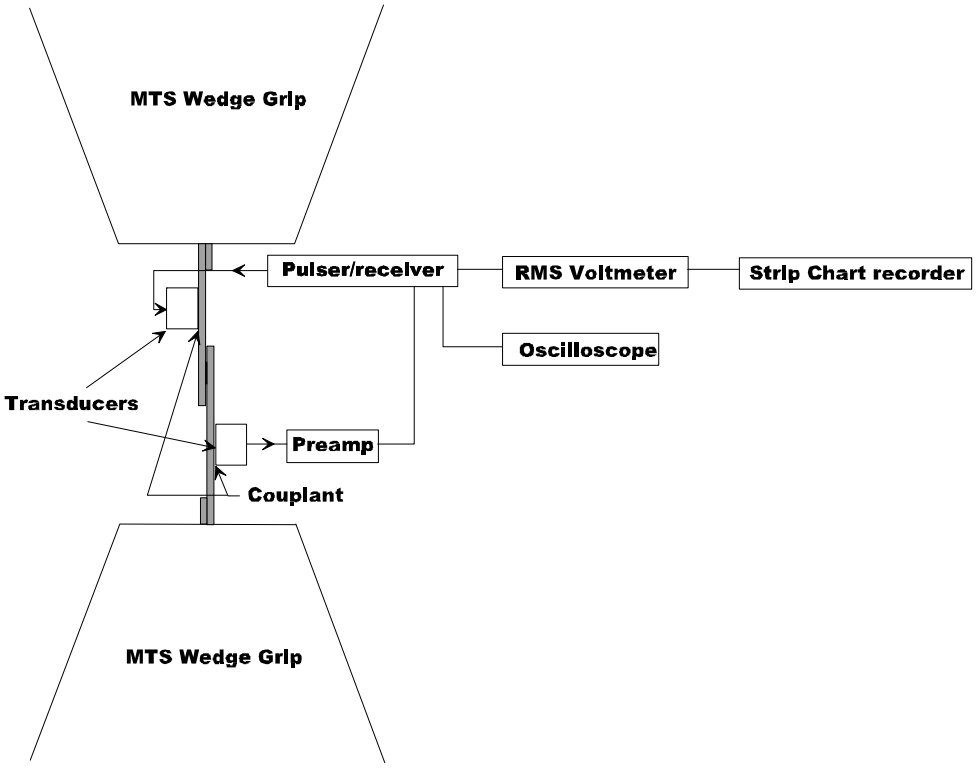


**Figure 2.2 Schematic of acousto-ultrasound fatigue setup.**

## *2.3 Radiography*

Radiography has long been used as a means of validating new nondestructive inspection methods. In this situation it was used as a means of attempting to validate the presence of a crack for the purpose of correlating the change in the AU signal due to the presence and propagation of the crack. The radiographs were performed on many specimens. Each specimen was exposed to 100 KeV for 2 minutes.

Along with normal radiographs, some specimens were injected with a penetrant, zinc iodide. Zinc iodide is used as an enhancement for radiographs by penetrating into the crack and revealing its presence in the radiograph. The two sheets of metal were pulled apart by applying a slight tensile load and the penetrant was then injected with a needle. Another technique used to apply the penetrant was to allow the spot weld to soak in the penetrant. It was thought that the fluid would more readily penetrate the crack if it were allowed to dwell for an extended time period. None of the specimens treated with zinc iodide were found to have any clearer radiographic indication than specimens not treated with the penetrant. Therefore, the use of zinc iodide was stopped.

## *2.4 Sectioning*

Sectioning was used as another means to validate the presence of a crack. By sectioning the samples, it was possible to accurately identify the presence and size of a crack. In the interest of providing a quantitative analysis of the crack presence and propagation, it was deemed necessary to attempt to measure the crack at its greatest length. This was accomplished by sectioning the welds vertically off center, mounting them in a polymer, and then polishing them, inspecting them, and repolishing them until they approached what appeared to be the maximum crack length. The specimens were first polished using progressively finer grits of sandpaper. A felt wheel and alumina oxide particles were then used to obtain a finer polish.

The mounting of the specimens was performed using a temperature-pressure process. First, the excess material around the spot welds was removed by cutting the specimen along A-A' and B-B' in Figure 2.4.1. From earlier experiments, it was found that the crack initially broke through the surface at points near the vertical center of the weld nugget, C and D in Figure 2.4.1, and then followed the circumference of the weld until failure. Therefore, it was determined that the initial sectioning of the spot weld would begin slightly off center, E-E'. The sectioned specimen was then mounted, polished, and repolished along E-E', until the maximum crack length was measured.

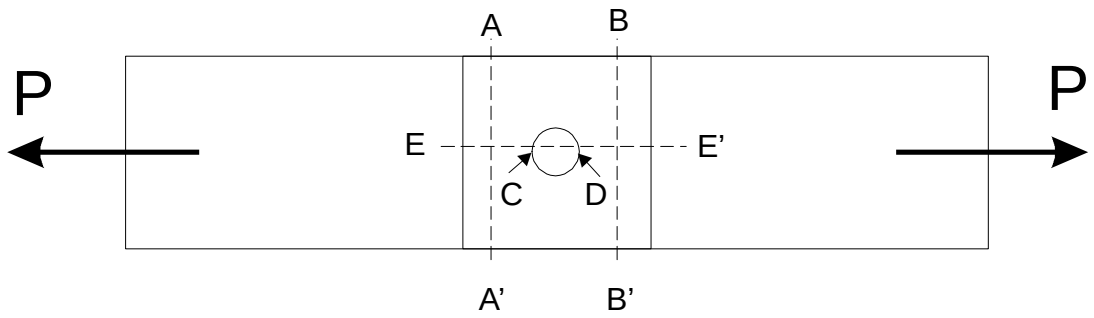


**Figure 2.4.1 Diagram of sectioning cuts where P represents direction of applied load.**

Specifically, the specimens were mounted in an acrylic by covering them with a powder formula and then applying heat and 4 ksi pressure until the acrylic cured. After cooling, the specimens were polished as described above.

The inspection of the specimens was performed under a microscope at magnifications ranging from 5X up to 100X. It was necessary to define an orientation for the specimens because the repeated polishings potentially would cause the crack appearance to change significantly. (It is common for the spot weld to have cracks at both edges of the weld.[(4)]) The orientation of the specimens was such that the mounting bracket used to hold the specimen in place while it was mounted in the acrylic was always oriented to be on the right edge of the specimen as it appeared under the microscope.

As can be seen from the pictures in Appendix A, the sectioning proved to be an effective means of verifying the presence of a crack. A reliable method of establishing crack length was essential for correlation changes in AU with crack length.

## 3. Results and Discussion

Since the nondestructive evaluation of the spot welds during fatigue was only one facet of this project, the available specimens were shared. The objective 4being to examine the spot welds during fatigue loading, the lap shear joints were cyclically loaded in an MTS servo-hydraulic machine. Some samples were run during the initial stages of the project in order to establish the static strength loads for both materials. This provided a basis for determining the load levels for the fatigue testing so as to achieve lives between $10^2$ and $10^6$ cycles. These load regimes ranged from approximately 30% to 90% of the static strength.

For the AU testing, however, the load regimes were between 40% and 60% for both the 1010 steel and the 950 X steel. These load regimes were chosen to provide a reasonable amount of data in a reasonable amount of time. Tables 3.1 and 3.2 list of all of the mild (1010) steel lap joint specimens tested, with those for which AU data were recorded being indicated by gray shading. If there is a column missing, that would indicate a lack of reliable data. This could be related to equipment failure, poor connections, or operator error. Tables 3.3 and 3.4 list similar data for the high strength (950X) steel lap joints.

Table 3.5 contains the data from the AU measurements and the sectioning. The sectioning data is listed under the column heading Max. Crack Length. These data are the result of multiple sectionings and polishings. The data portrayed are

**Table 3.1 1010 Steel – Batch 1**

| Specimen | Max. Load (lbf) | Load Ratio | Rate (Hz.) | First Crack (cycles) | ¼ circ. (cycles) | Failure (cycles) |
|---|---|---|---|---|---|---|
| L1-101 | 1823 | | | Static Test | | 1 |
| L1-103 | 900 | 0.1 | 10 | 6,000 | 11,500 | 25,499 |
| L1-104 | 900 | 0.1 | 10 | 12,000 | 18,000 | 30,511 |
| L1-105 | 650 | 0.1 | 10 | 23,000 | 46,000 | 109,563 |
| L1-106 | 470 | 0.1 | 10 | 21,000 | 35,000 | 534,000 |
| L1-107 | 470 | 0.1 | 10 | 107,000 | 210,000 | 466,753 |
| L1-108 | 350 | 0.1 | 10 | 794,000 | 1,424,000 | 2,285,178 |
| L1-109 | 1150 | 0.1 | 10 | 8,000 | 9,500 | 9,663 |
| L1-110 | 350 | 0.1 | 10 | 575,000 | 932,000 | 1,555,650 |
| L1-111 | 1150 | 0.1 | 10 | | | 8,225 |
| L1-112 | 1150 | 0.1 | 10 | | | 7,612 |
| L1-113 | 900 | 0.1 | 10 | | | 26,000 |
| L1-114 | 900 | 0.1 | 10 | | | 26,000 |
| L1-115 | 900 | 0.1 | 10 | | | 26,000 |
| L1-116 | 900 | 0.1 | 10 | | | 26,000 |
| L1-117 | 900 | 0.1 | 10 | | | 26,000 |
| L1-118 | 1150 | 0.1 | 10 | | | 8,500 |
| L1-119 | 1150 | 0.1 | 10 | | | 8,500 |
| L1-120 | 1150 | 0.1 | 10 | | | 8,500 |
| L1-121 | 900 | 0.1 | 10 | | | 22,681 |
| L1-122 | 1150 | 0.1 | 10 | | | 8,500 |
| L1-123 | 1150 | 0.1 | 10 | | | 8,500 |
| L1-124 | 1150 | 0.1 | 10 | | | 8,500 |
| L1-125 | 1200 | 0.1 | 10 | | | 11,000 |

**Table 3.2 1010 Steel – Batch 2**

| Specimen | Max. Load (lbf) | Load Ratio | Rate (Hz.) | First Crack (cycles) | ¼ circ. (cycles) | Failure (cycles) |
|---|---|---|---|---|---|---|
| L1-203 | 1700 | | | Static Test | | 1 |
| L1-204 | 1680 | | | Static Test | | 1 |
| L1-205 | 600 | 0.5 | 10 | 400,000 | 475,000 | 502,987 |
| L1-206 | 800 | 0.5 | 5 | 220,000 | | 242,420 |
| L1-207 | 1000 | 0.5 | 10 | | | 77,972 |
| L1-208 | 600 | 0.1 | 10 | | 100,000 | 100,042 |
| L1-209 | 1200 | 0.5 | 1 | 62,000 | | 62,165 |
| L1-210 | 400 | 0.5 | 20 | | | >6,800,000 |
| L1-211 | 1300 | 0.5 | 3 | | | 46,300 |
| L1-212 | 800 | 0.75 | 30 | | | >6,800,000 |
| L1-213 | 1200 | 0.75 | 10 | 640,000 | 670,000 | 682,433 |
| L1-216 | 1300 | 0.75 | 10 | 550,000 | 580,000 | 580,237 |
| L1-217 | 1400 | 0.75 | 5 | 315,000 | | 324,050 |
| L1-218 | 1200 | 0.1 | 5 | 11,000 | | 11,607 |
| L1-219 | 1400 | 0.1 | 10 | 5,200 | 5,300 | 5,325 |
| L1-220 | 500 | 0.5 | 30 | | | >6,800,000 |
| L1-221 | 400 | 0.1 | 10 | 450,000 | 475,000 | 483,004 |
| L1-222 | 1250 | 0.1 | 10 | 11,400 | 11,600 | 11,686 |
| L1-223 | 1500 | 0.1 | 10 | 680 | 688 | 694 |
| L1-224 | 550 | 0.5 | 30 | | | 2,809,075 |
| L1-225 | 1600 | 0.75 | 10 | 342 | 342 | 342 |
| L1-231 | 1200 | 0.1 | 10 | | | 7475 |

**Table 3.3 950X Steel – Batch 1**

| Specimen | Max. Load (lbf) | Load Ratio | Rate (Hz.) | First Crack (cycles) | ¼ circ. (cycles) | Failure or Stopped (cycles) |
|---|---|---|---|---|---|---|
| L9-101 | 2654 | | | | | 1 |
| L9-103 | 950 | 0.1 | 10 | | | 18,946 |
| L9-104 | 950 | 0.1 | 10 | | | 20,277 |
| L9-105 | 1300 | 0.1 | 10 | | | 6,091 |
| L9-106 | 500 | 0.1 | 10 | | | 224,157 |
| L9-107 | 500 | 0.1 | 10 | | | 296,300 |
| L9-108 | 370 | 0.1 | 10 | 30,000 | 365,000 | 407,968 |
| L9-109 | 1300 | 0.1 | 10 | 4,000 | 5,000 | 6,355 |
| L9-110 | 700 | 0.1 | 10 | 14,000 | 45,000 | 67,653 |
| L9-111 | 700 | 0.1 | 10 | 11,200 | 32,000 | 53,350 |
| L9-112 | 370 | 0.1 | 10 | 450,000 | 650,000 | 759,879 |
| L9-114 | 1300 | 0.1 | 10 | | | 2,000 |
| L9-118 | 1300 | 0.1 | 10 | | | 4,500 |
| L9-119 | 950 | 0.1 | 10 | | | 10,000 |
| L9-120 | 950 | 0.1 | 10 | | | 12,000 |
| L9-121 | 950 | 0.1 | 10 | | | 6,800 |
| L9-122 | 950 | 0.1 | 10 | | | 5,100 |
| L9-124 | 950 | 0.1 | 10 | | | 850 |
| L9-125 | 950 | 0.1 | 10 | | | 2,550 |

**Table 3.4 950X Steel – Batch 2**

| Specimen | Max. Load (lbf) | Load Ratio | Rate (Hz.) | First Crack (cycles) | ¼ circ. (cycles) | Failure or Stopped (cycles) |
|---|---|---|---|---|---|---|
| L9-201 | 2030 | | | | | 1 |
| L9-202 | 2060 | | | | | 1 |
| L9-204 | 1000 | 0.5 | 10 | 58,000 | 63,000 | 63,591 |
| L9-205 | 1200 | 0.5 | 10 | 27,000 | 31,000 | 31,863 |
| L9-206 | 800 | 0.5 | 10 | 165,000 | 180,000 | 190,296 |
| L9-207 | 600 | 0.5 | 10 | 490,000 | 525,000 | 555,228 |
| L9-208 | 400 | 0.5 | 20 | 3,600,000 | | 4,071,942 |
| L9-209 | 1400 | 0.5 | 5 | 17,000 | 19,000 | 19,400 |
| L9-213 | 1200 | 0.1 | 10 | | | 4,985 |
| L9-215 | 1200 | 0.1 | 10 | 6,700 | 6,743 | 6,743 |
| L9-216 | 1100 | 0.1 | 10 | | | 5,543 |
| L9-217 | 1100 | 0.1 | 10 | 5,700 | 5,804 | 5,804 |
| L9-218 | 1000 | 0.1 | 10 | | | 7,448 |
| L9-221 | 1800 | 0.5 | 10 | 2,270 | 2,270 | 2,270 |
| L9-222 | 1800 | 0.1 | 10 | 454 | 454 | 454 |
| L9-223 | 350 | 0.1 | 25 | | | 968,419 |
| L9-224 | 1600 | 0.1 | 10 | 1,297 | 1,297 | 1,297 |
| L9-225 | 1600 | 0.75 | 20 | 126,000 | 131,000 | 131,749 |
| L9-226 | 1800 | 0.75 | 20 | 61,000 | 61,042 | 61,042 |
| L9-227 | 1200 | 0.75 | 25 | | | 380,354 |

**Table 3.5 Maximum Crack Length and AU Change**

| Specimen | Load Range | Expected Life | Stopped | % of Life | % AU Change | Max. Crack Length, μm |
|---|---|---|---|---|---|---|
| L1-111 | 1150-115 | 8225 | --- | 100 | 84 | |
| L1-112 | 1150-115 | 7612 | --- | 100 | 91 | |
| L1-113 | 900-90 | 26000 | 9100 | 35 | 8 | 140 |
| L1-114 | 900-90 | 26000 | 7800 | 30 | 27 | 160 |
| L1-115 | 900-90 | 26000 | 10400 | 40 | 9 | 230 |
| L1-116 | 900-90 | 26000 | 13000 | 50 | 10 | 250 |
| L1-117 | 900-90 | 26000 | 18000 | 70 | 6 | 560 |
| L1-118 | 1150-115 | 8500 | 3500 | 41 | 29 | 130 |
| L1-119 | 1150-115 | 8500 | 3500 | 41 | 24 | 65 |
| L1-120 | 1150-115 | 8500 | 4750 | 56 | 28 | 140 |
| L1-121 | 900-90 | 22681 | --- | 100 | 93 | |
| L1-122 | 1150-115 | 8500 | 4750 | 56 | 45 | 500 |
| L1-123 | 1150-115 | 8500 | 7125 | 84 | 40 | 520 |
| L1-124 | 1150-115 | 8500 | 7125 | 84 | 75 | 1000 |
| L1-125 | 1200-120 | 11000 | 4500 | 41 | 33 | 570 |
| L9-114 | 1300-130 | 6200 | 2000 | 32 | | 150 |
| L9-118 | 1300-130 | 6200 | 4500 | 73 | 25 | 520 |
| L9-119 | 950-95 | 18000 | 10000 | 56 | 12 | 460 |
| L9-120 | 950-95 | 18000 | 12000 | 67 | 62 | 630 |
| L9-121 | 950-95 | 18000 | 6800 | 38 | 7 | 360 |
| L9-122 | 950-95 | 18000 | 5100 | 28 | ? | 160 |
| L9-125 | 950-95 | 18000 | 850 | 5 | 11 | 45 |
| L9-126 | 950-95 | 18000 | 2550 | 14 | 6 | 49 |

the maximum crack lengths measured from either side of the weld (top or bottom, left or right). The measurements are in microns and were measured by using a micrograph of a 1000 μm scale magnified at appropriate scales (5X, 10X, 20X, and 50X). The percent change in the AU signal is a measurement which has been normalized. The signal measurement came from the RMS voltmeter and has been converted to a percentage change by dividing the initial signal value by the final signal value and subtracting that value from 1. This method was used in order to calculate a relative percentage change for each individual specimen, as the initial AU signal may not have been identical for each specimen. Figure 3.1 shows a typical measurement of the AU signal as an RMS voltage. This particular sample is L9-120, 950 lb. maximum load, R = 0.1, at 10 Hz.

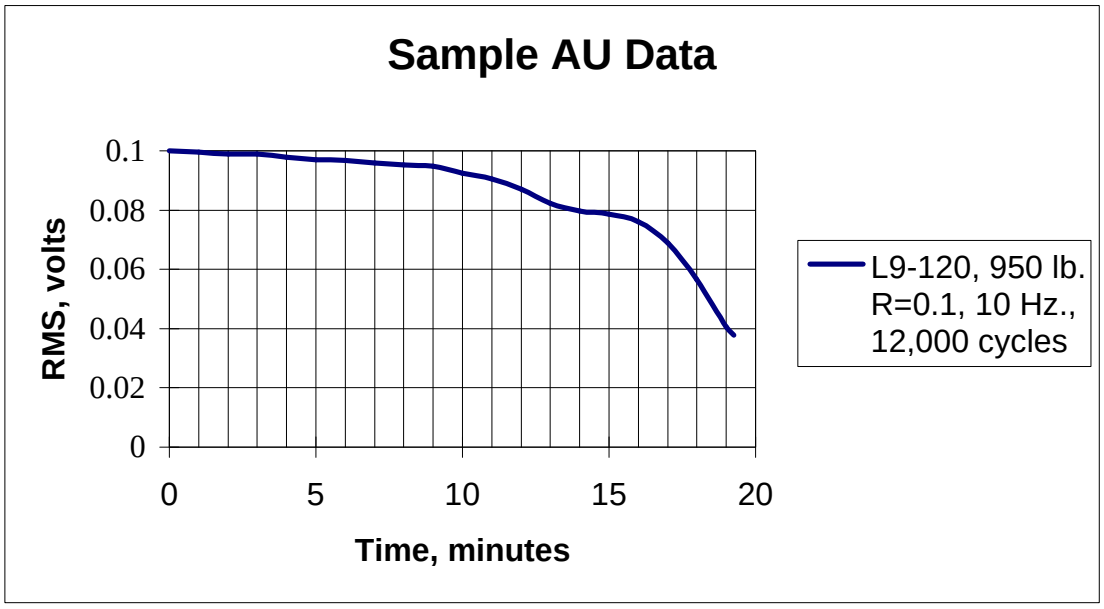


**Figure 3.1 Example of a typical AU measurement.**

The percentage of life was determined as a function of the average of previously tested to failure specimens at specific load levels. As not every specimen is the same, it was concluded that it would be best to use an average value for the expected life. This value was used for evaluating the percentage of life at which to stop the fatigue cycling and section the specimen. This procedure leaves a window of uncertainty in the calculations as to the exact percent of life. The significance of these assumptions will be discussed later.

The change in the AU signal measurements are affected by different factors, such as a flaw or discontinuity (crack), the material itself, and geometry. Another cause for variation in the strength of the AU signal is the size and placement of the transducer. If the transducer is larger than the weld nugget by a considerable amount, it is conceivable that the signal degradation by a crack would be small. Similarly, if the transducer were smaller than the weld nugget, and a crack formed and grew in the manner suggested, then it is possible the stress wave propagation path might not intersect with the crack. However, if the general path of the stress wave did intersect the crack front, there would be a much greater influence due to the crack. From this reasoning, it was decided that the width selected for the transducer should be the same width as the diameter of the weld. The commercially available transducer used in these experiments was very close to the same width as the weld nuggets being tested.

Transducer placement was another area of concern. In order to evaluate the condition of the weld and the heat affected zone, it was necessary for the sound wave to travel through the welded region. In conventional acousto-ultrasound, the receiving transducer is normally placed on the same surface as the transmitting transducer.[5,8,14] However, the geometrical constraints of the samples prohibited this. The transducer was ¾ of an inch in length and the amount of metal on the short side of the weld was only 7/16 of an inch long. As mentioned earlier, Rokhlin, Meng, and Adler showed that the welding of two strips of metal insures the transmission of an incident wave from one sheet to the other.[3] So, for this situation, it was determined that the optimal configuration would be opposite sheets of metal.

### *3.1 AU v. Crack Length*

As stated before, the objective of this project was to determine if a correlation existed between the degradation of the spot weld due to fatigue and a means by which to assess the damage. The data obtained from the AU signal and the sectioning implies a significant correlation between the AU signal and the maximum crack length. As mentioned earlier, there have been three stages documented in the fatigue life of spot welds. During Stage I, the crack initiates and experiences early crack growth; during Stage II, it propagates up through the thickness of the weld and into the base metal; and finally, in Stage III, it breaks through the surface and propagates across the face of the specimen in an "eyebrow" manner.[4,17]

Swellam, et al. concluded that Stage I had accounted for approximately 40% of the life of low carbon steel specimens whose lives were in the range of $10^5 – 10^7$ cycles.[4] McMahon, et al. showed that for high strength steel specimens with lives between $10^4$ and $10^6$ cycles that approximately 50% of the life was spent in Stage I developing a 0.25mm crack.[17] These conclusions are consistent with some of the findings in this study as well.

As can be seen in Figures 3.1.1, 3.1.2, and 3.1.3, the crack length increases with an increase in the percent of life, but at different rates for different load levels and material. This is observed in the least squares fit equation attached to each graph. The slopes of the lines are slightly different which indicates that the increase in crack length is load level and material dependent.

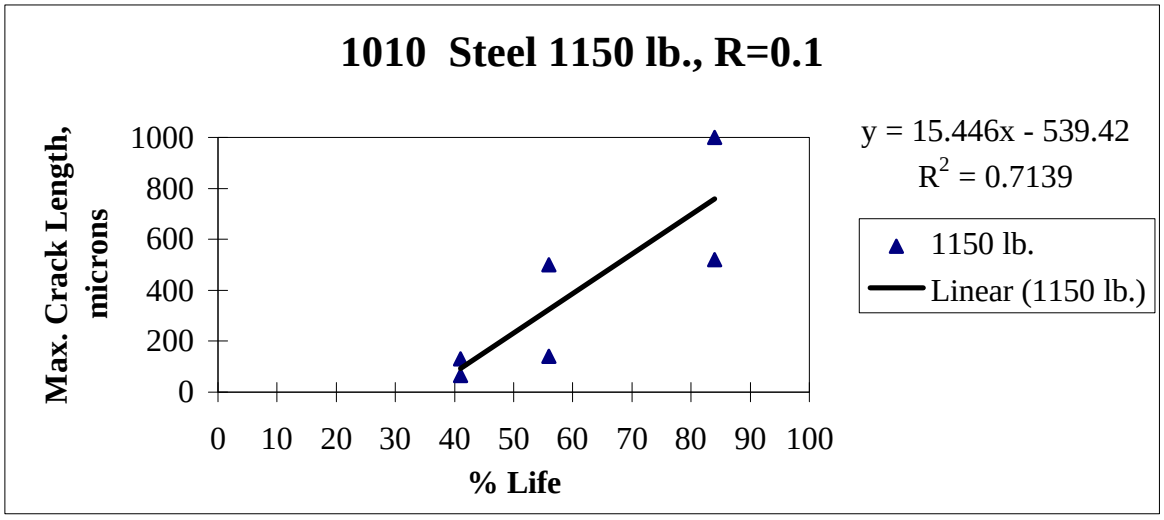


**Figure 3.1.1 Life v. Crack length correlation for 1150 maximum load, R=0.1, 1010 steel.**

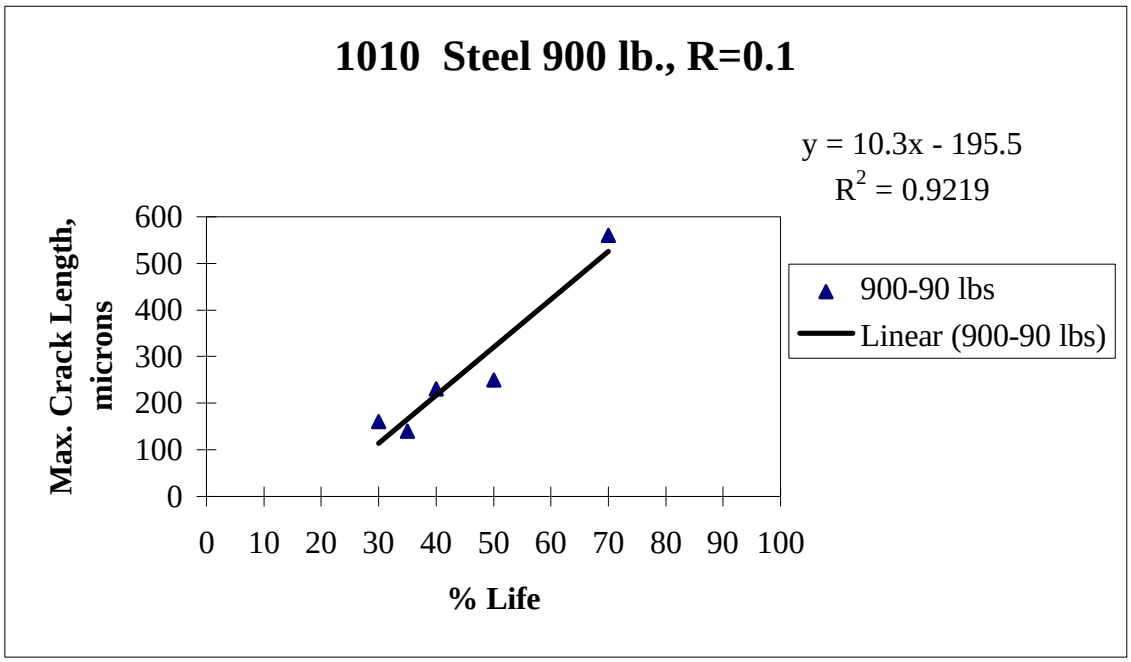


**Figure 3.1.2 Life v. Crack length correlation for 900 lb. maximum load, R=0.1, 1010 steel.**

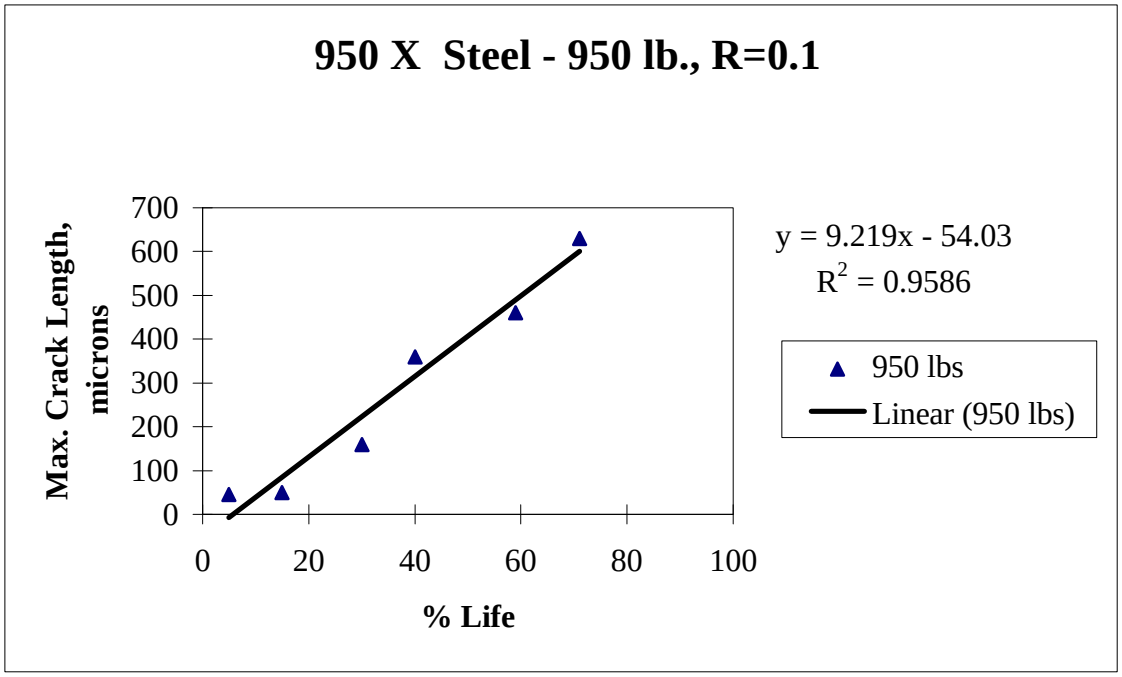


**Figure 3.1.3 Life v. Crack length correlation for 950 lb. maximum load, R=0.1, 950X steel.**

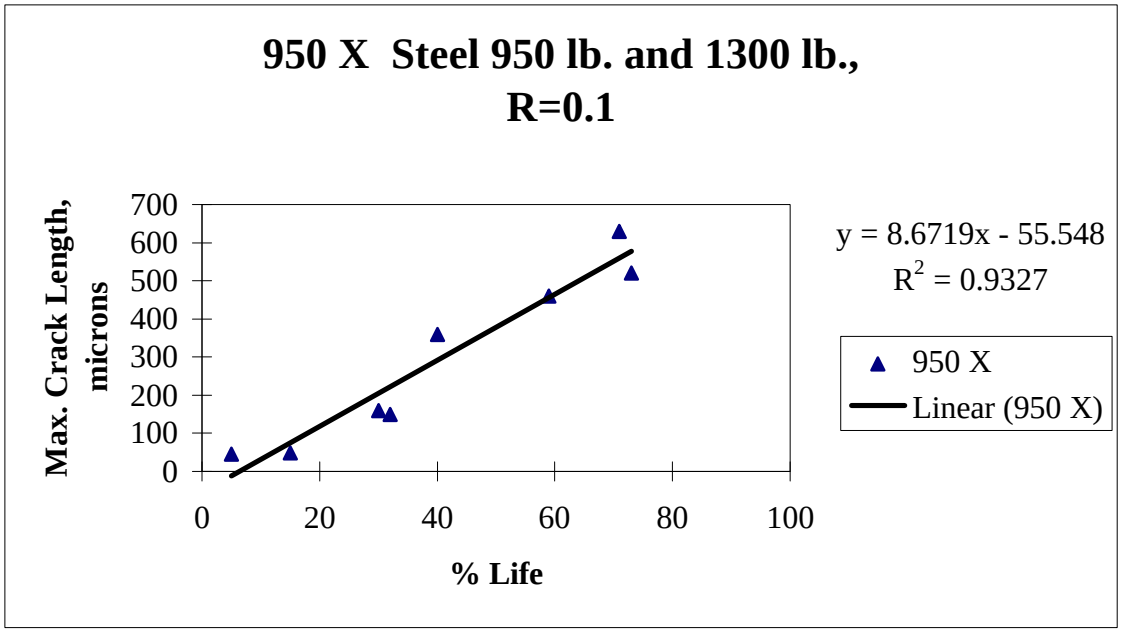


**Figure 3.1.4 Life v. Crack length correlation for both 950 lb. and 1300 lb. maximum load, R=0.1, 950X Steel.**

It can be seen in Appendix A that specimen L9-125 has a very small crack in it. This specimen was only tested to 5% of its life. A crack is also present in specimen L9-126 at 15% of its life. These crack lengths were measured to be 45 and 49 microns, respectively. This is only a small fraction of the 1 mm thickness of the weld. This would indicate that the detection of a crack during the very early stages of the fatigue life is possible and that perhaps Lawrence's choice of an arbitrarily small initiating crack length could be even smaller decreasing the percentage of life devoted to initiating a crack.

### *3.2 AU v. Percent Life*

The presence of a crack in the specimen usually leads to failure. It has been shown that the presence of a crack has an effect on the amount of ultrasonic stress wave energy that passes through the weld. As the crack grows, a smaller amount of energy passes through the weld which suggests that the crack is attenuating the signal. Crack growth is the primary mechanism of failure in the spot welded specimen and thus is related to the fatigue life of the specimen. As can be seen in Figure 3.2.1, there exists a strong correlation between the change in the AU signal and the percent of life for the 1010 steel at a 1150 lb. maximum load. In Figure 3.2.2, the correlation is considerably weaker, but shows the tendency towards an exponential fit and could be better supported with more data. These results shows that it is possible the AU signal could be eventually used to monitor the damage progression in a spot welded specimen.

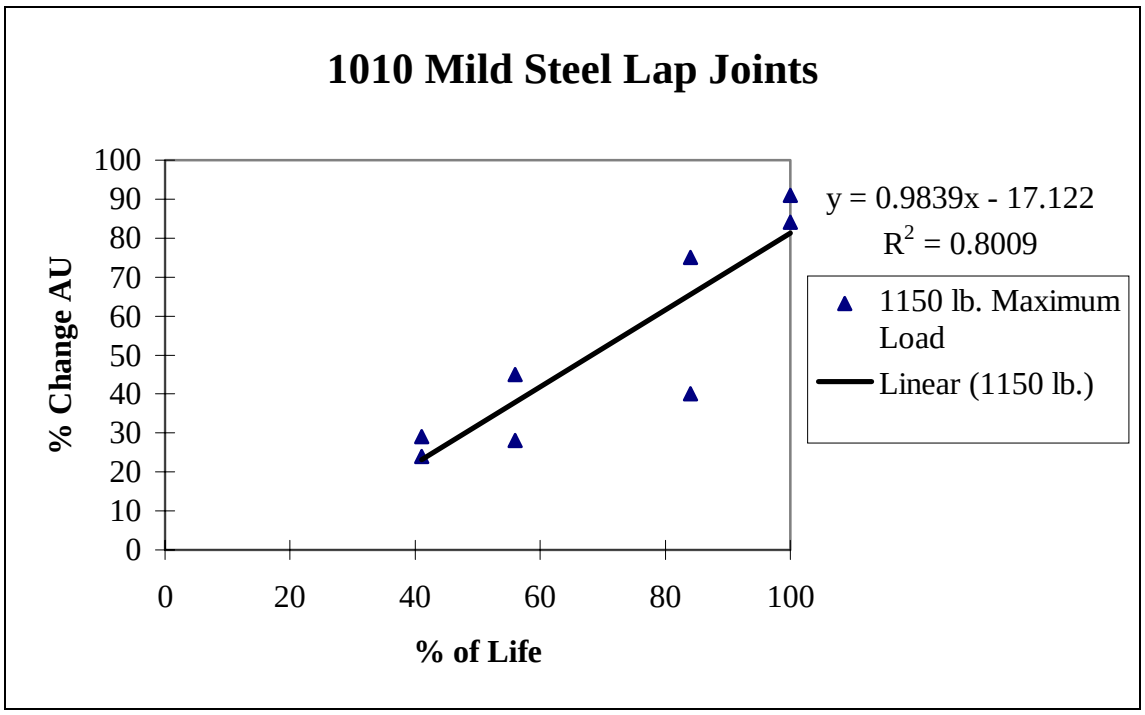


**Figure 3.2.1 Trend between % Change in AU and % of Life for 1150 lb. maximum load, R=0.1, 1010 steel.**

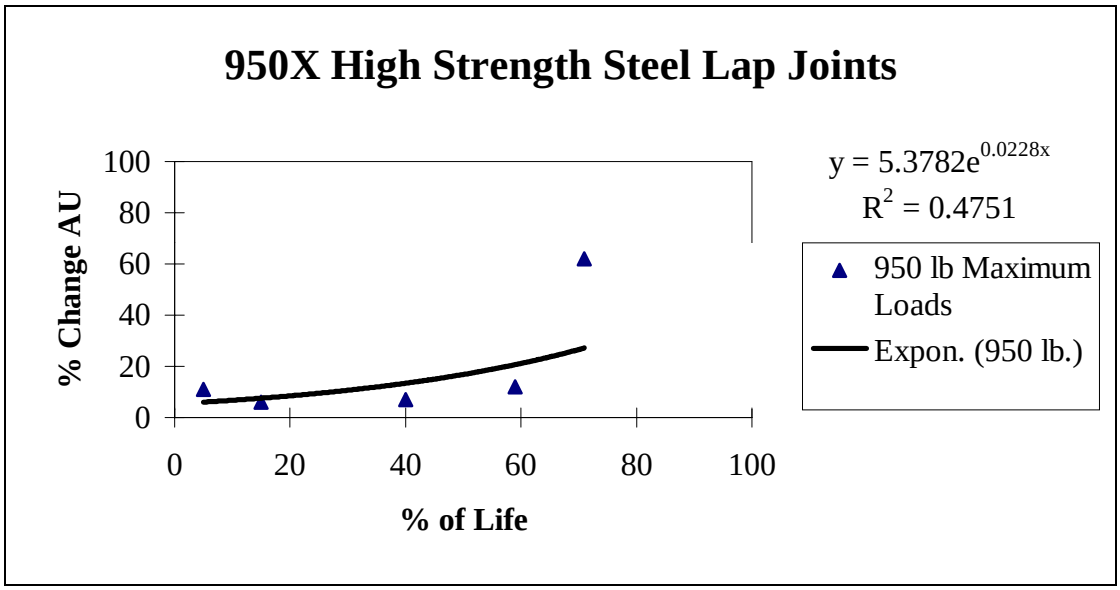


**Figure 3.2.2 Trend between % Change in AU and % of Life for 950 lb. maximum load, R=0.1, 950X steel.**

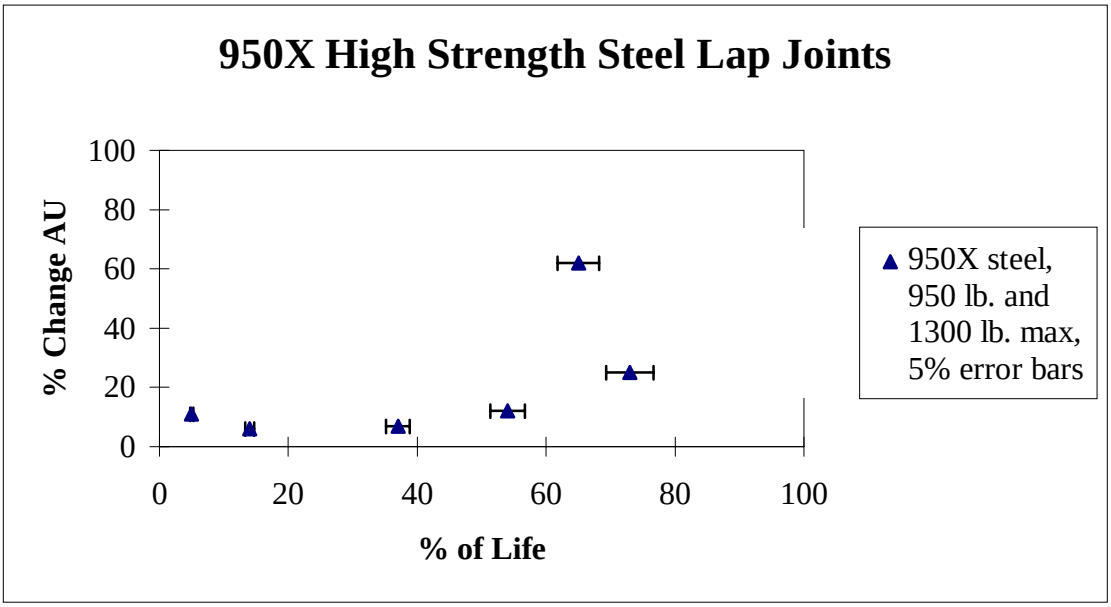


**Figure 3.2.3 Plot showing percent error based on life range.**

As mentioned earlier, the assumptions made on the expected life may have an effect on the data interpretation. As shown in Figure 3.2.3 there exist approximately a ± 5% error in the expected lives of the specimens causing some overlap as seen in the last two data points. This could affect the fit of a line to this data. The error bars were calculated by ranging the expected life between the shortest fatigue life tested and the longest fatigue life tested.

### *3.3 Energy*

As stated before, the underlying principle of acousto-ultrasound is the efficiency of energy transmission. The signal received by the transducer is related to energy that has passed through the weld region. A discontinuity or crack will cause scattering and diffraction of a portion of that energy resulting in a lower detected energy envelope. As the crack size increases, the amount of energy transmitted decreases.

Crack formation is three dimensional. So, as the crack grows the larger surface area of the crack face causes more dispersion of the impinging stress wave resulting in a lower transmitted signal. As the crack enters stage II it is propagating from the spot weld into and through the HAZ toward the base metal at an approximate angle of 60° with the horizontal, as can be seen in Figure 3.31.[,17] This angle will cause a direct interference with the stress wave propagating from one sheet to the other. Many of the specimens tested resulted in similar findings to Figure 3.3.1 below. More micrographs can be found in Appendix A.

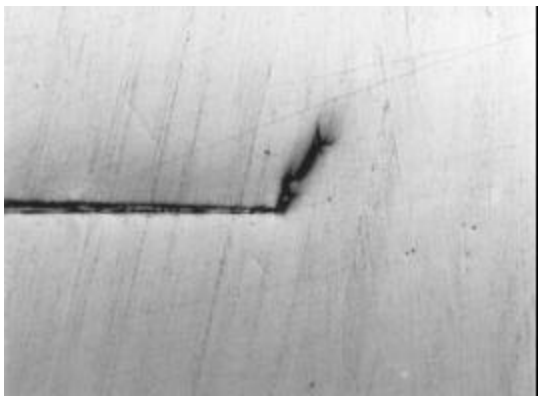

**Figure 3.3.1 Micrograph of fatigue crack showing the angle of propagation.**

Figure 3.3.2 and Figure 3.3.3 are plots of the percent change in AU signal versus the maximum crack length for the 1010 mild steel, for load levels of 1150lbs. and 900 lbs. respectively. It can be seen that there is a progressive trend such that the change in AU signal increases as the crack length increases for the 1150 lb. load level. In the 900 pound load regime, however, the trend does not appear to be as clear. Perhaps one explanation for the lack of AU changes as the crack length increases is the possibility that as the specimen is being tested, the crack is opening and closing completely. If the crack face is closing completely when the load decreases, this would allow more of the signal to transmit through the weld and the crack. It was expected that at this load level as the crack length proceeded to near 75% of the thickness of the sheet metal, the AU signal would begin to change more rapidly. More testing would verify these hypotheses.

Another possible explanation for the lack of a trend is based on the work by McMahon, et al. They showed that for specimens whose fatigue lives ranged from $10^4$ to $10^6$ cycles that approximately 50% of their lives were spent developing a 0.25mm crack.[17] According to Figure 3.1.2, it would appear that the 900 lb. load level for 1010 mild steel data supports their findings.

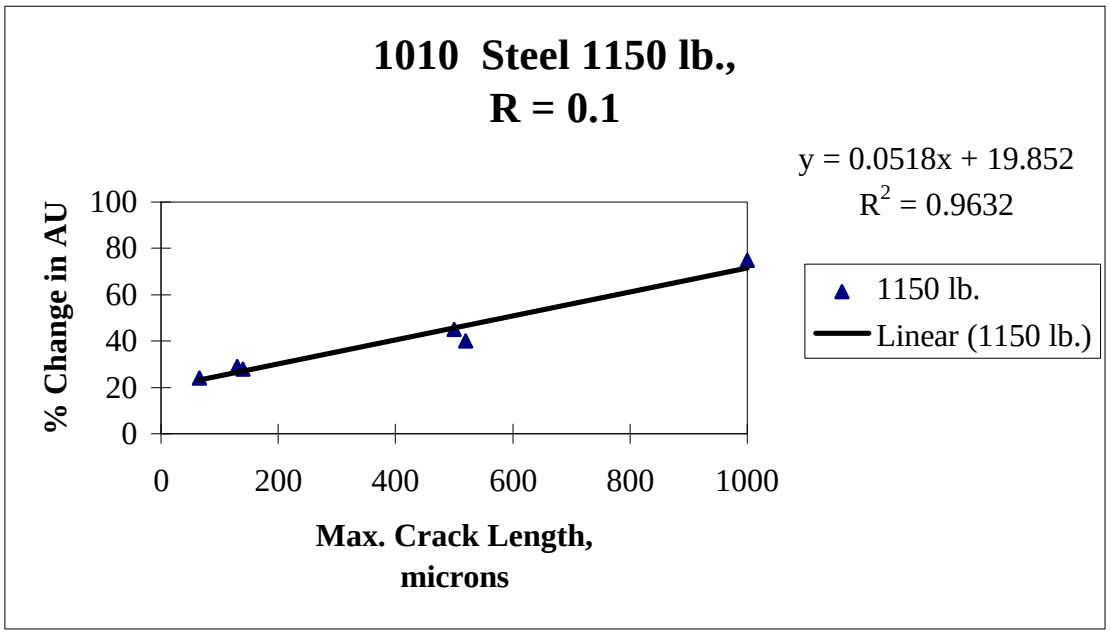


**Figure 3.3.2 Correlation between % Change in AU and Maximum crack length for 1010 Steel 1150 lb. maximum load, R=0.1.**

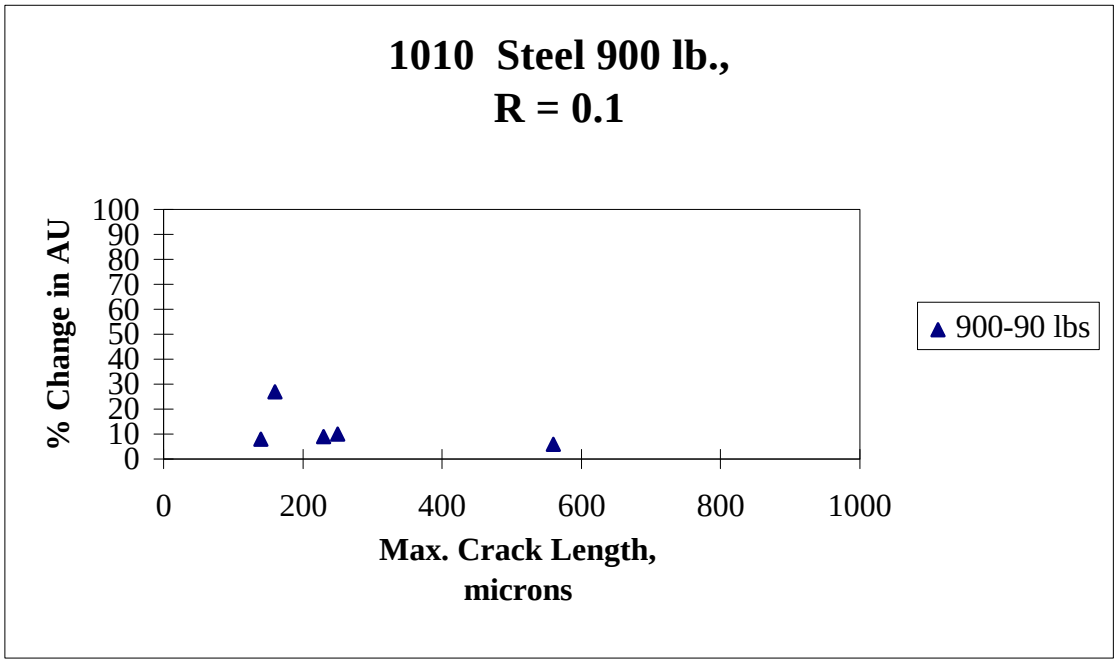


**Figure 3.3.3 Correlation between % Change in AU and Maximum crack length for 1010 Steel 900 lb. maximum load, R=0.1.**

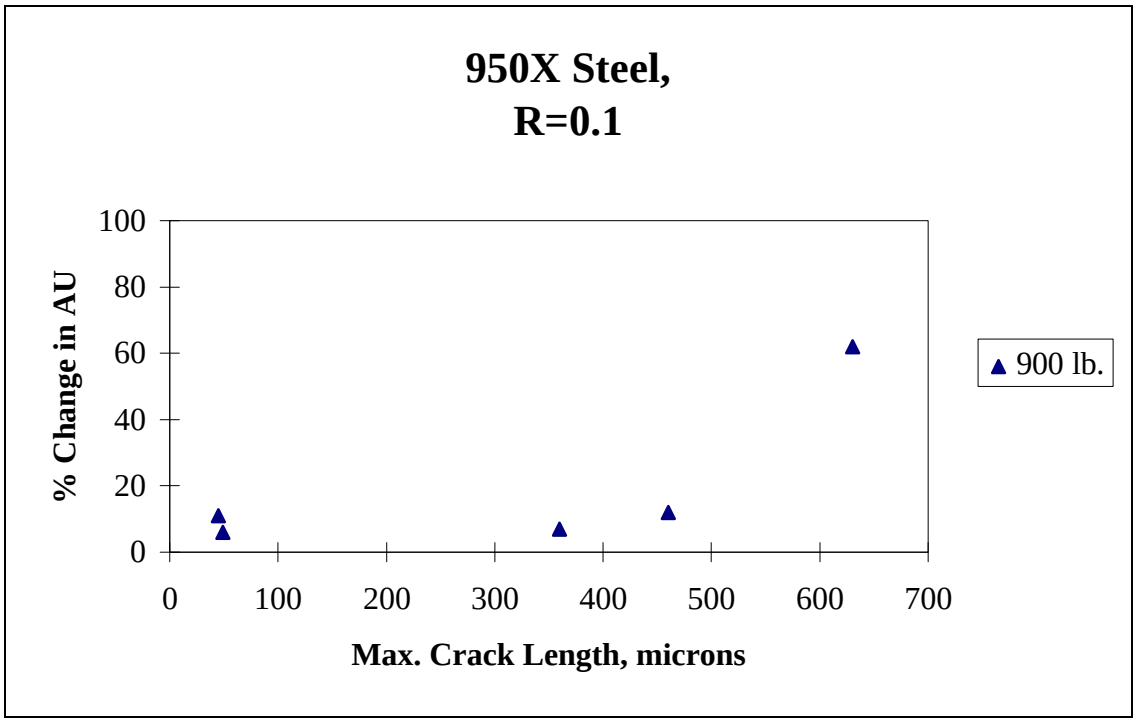


**Figure 3.3.4 Percent Change in AU v. Maximum Crack Length for 950X steel.**

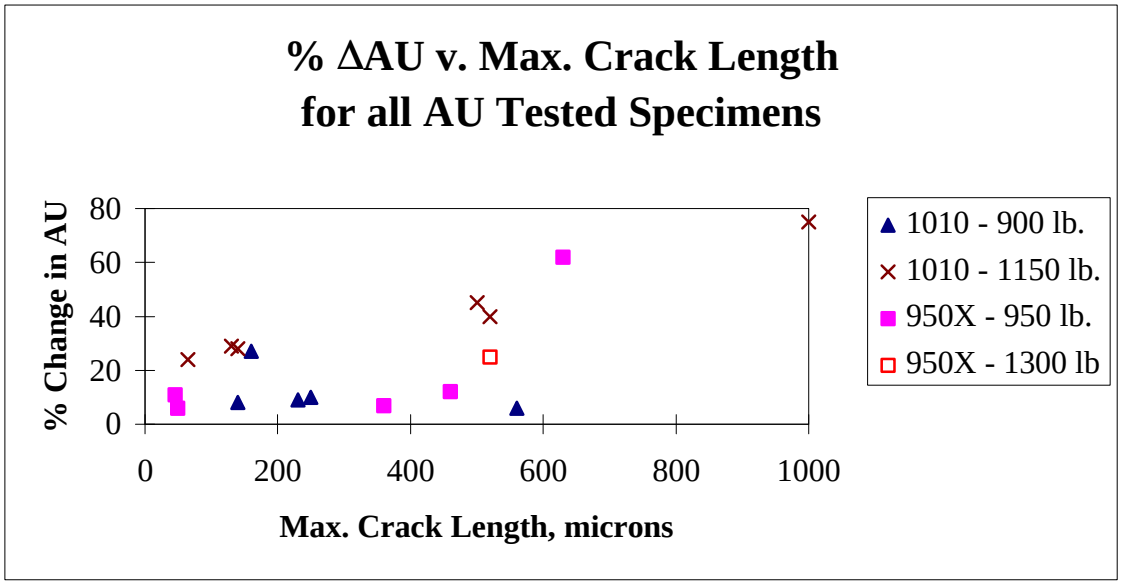


**Figure 3.3.5 Combined plot of both materials and all load levels.**

Figure 3.3.4 is a plot of percent change in AU versus maximum crack length. The data indicates at this load level that there's not much change in AU until the crack grows to a length of approximately 500 microns. The plot shows what appears to be an exponential growth. In order to verify this, more tests would need to be run at intermediate points and between 60 percent change and failure.

Figure 3.3.5 is a plot of all of the data for which AU was available. This plot supports the assumption that the relationship between the change in AU and maximum crack length is both material and load level dependent. The different materials and load levels are designated by different symbols. There does not seem to be a trend among all the specimens, but when viewed separately as shown in the previous graphs, there appears to be some correlations between the different sets of data.

The presence of a crack on both edges of the weld proved to be another interesting observation on many specimens. The two graphs in Figures 3.3.6 and 3.3.7 show this data as series marked left and right cracks. Not all the specimens had cracks present on both edges. The ones which did and were measured are shown in the figures below. For the 900 lb. load, there are three pairs of data which have cracks present at both edges. The data pair at the 40% change in AU shows that although the maximum crack length is only 180 microns, the significant change in AU may be due to the presence of the crack at

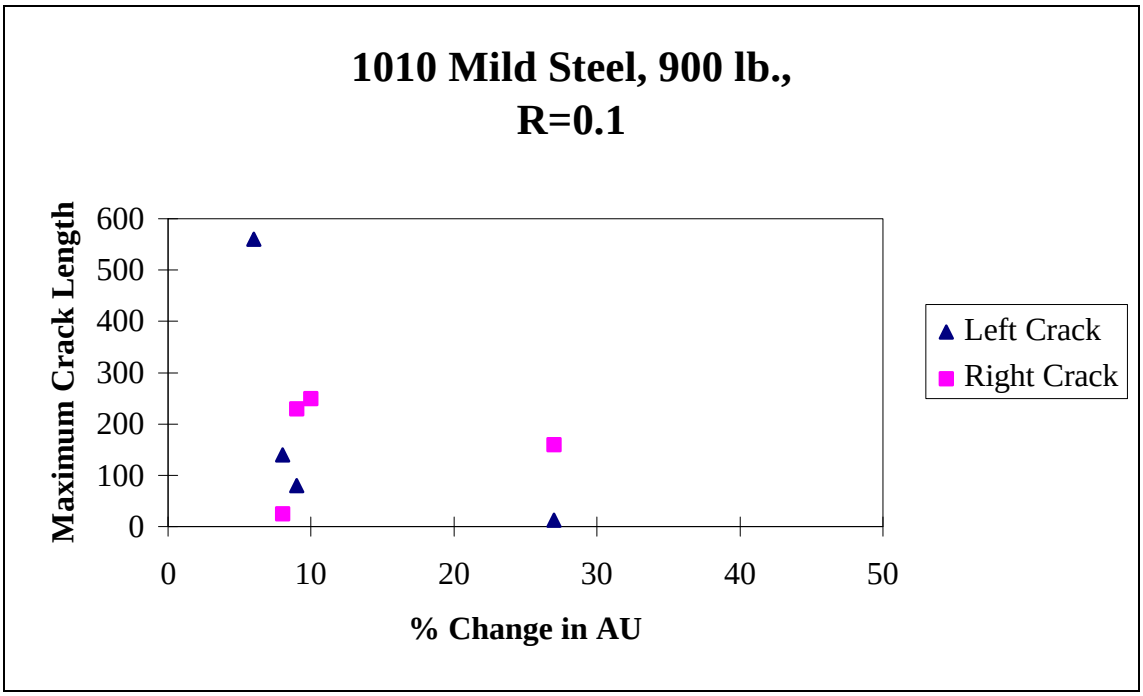


**Figure 3.3.6 Maximum Crack length on left and right sides for 1010 mild steel, 900 lb. maximum load, R=0.1.**

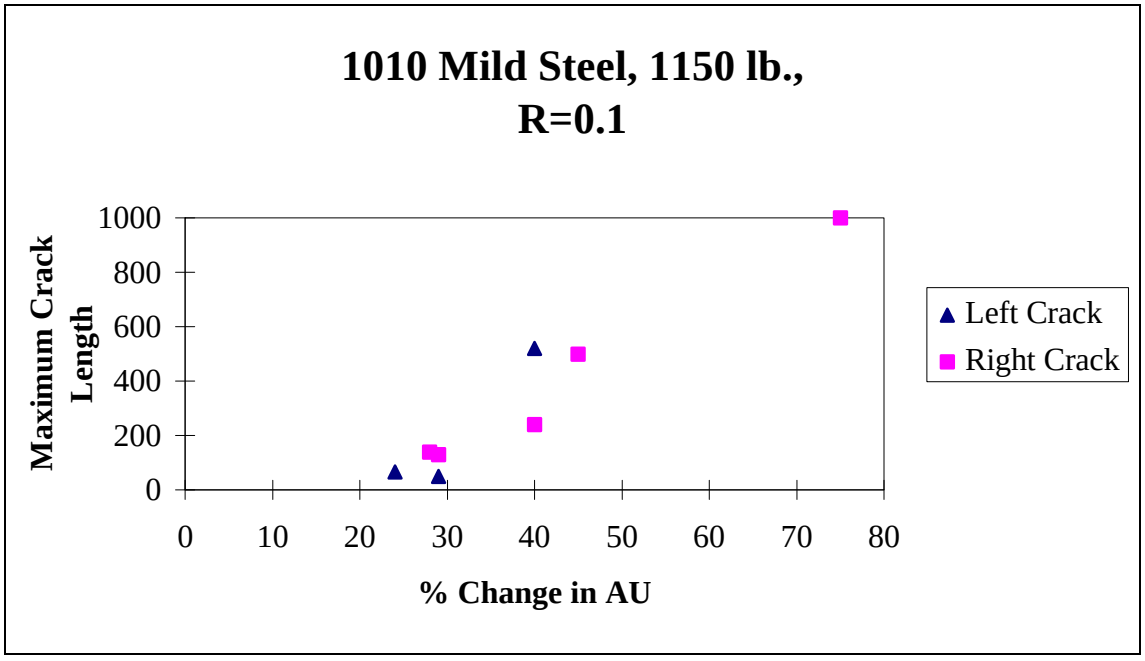


**Figure 3.3.7 Maximum Crack length on left and right sides for 1010 mild steel, 1150 lb. maximum load, R=0.1.**

the other edge of the weld. However, this data pair could be considered scatter relative to the two pairs of data in the 150-250 micron maximum crack length range which both have cracks present at both edges of the weld, yet the change in AU is not as dramatic as the first pair mentioned. Also, looking at Figure 3.3.7 the data pairs which have cracks present at both edges of the weld do not vary significantly in the percent change in AU relative to those which have only one crack present and a similar maximum crack length. This would indicate that the primary effect on the change in AU is due to the largest crack. It would be beneficial, however, to do a more in depth study on this phenomenon.

## 4. Conclusions

The objective of this project was to determine an effective method for nondestructively monitoring damage development of cyclically loaded spot welded members. After several attempts with different NDE methods, acousto-ultrasonics was chosen because it offered the greatest potential for successfully correlating a quantifiable signal to the presence of degradation of the specimen.

The acousto-ultrasound evaluation of the cyclic loading of spot welded specimens led to the following conclusions:

- A strong linear correlation ($R^2 = 0.9632$ ) exists between the change in AU signal and the crack length for 1010 steel, maximum load of 1150 lb., R = 0.1
- The correlation between change in AU and crack growth due to cyclic loading appears to be load dependent for mild steel
- The correlation between the change in AU and percentage of life could be used to determine damage development in prototype part testing
- AU observations did not refute the theory that a crack initiates at the onset of cycling
- Sectioning provided evidence that the AU data were due to crack growth
- Change in AU and crack growth rate also appear to be load level dependent

It is the belief of the author that the method tested here has produced evidence which would allow one to consider AU as a viable means by which to monitor the condition of spot welds under cyclic loading warranting further research.

## 5. Future Work

Spot welded structures are an invaluable part of the automotive industry and most likely will remain so in the near future. An ever-present issue will be the monitoring and evaluation of the performance of the spot welds. Researchers and manufacturers are striving to obtain a reliable method for detecting flaws and material degradation before catastrophic failure. Nondestructive evaluation and testing can be an extremely effective means by which to achieve this goal. In this project, it is the belief of the author that the results shown here have given sufficient evidence to suggest that acousto-ultrasonics may be a nondestructive method capable of accurately detecting fatigue crack propagation before the crack reaches the exterior surface and causes failure of a structural member.

Given the additional resources such as more specimens, funding, and support, it is reasonable to assume a better correlation could be found between a change in AU signal and the presence of material degradation, i.e. crack initiation and growth. Further studies may include running many duplicate tests. This would aid in filling in the gaps in the "% Change in AU v. Crack Length" curve to obtain a more statistically reliable mathematical representation. Also, the data obtained in this report suggest that not only is the crack length load level dependent, but that the corresponding change in AU signal is as well. By running more tests at different load regimes, this hypothesis could be quantified.

It is also the belief that this research has produced sufficient results to experimentally establish the capability of AU to be used to evaluate spot welds. The next logical step would be to do some more monitoring and experiments to establish a mathematical model to describe the exact nature of the AU signal and its interaction with the crack.

To address the possibility of loss of signal due to the crack opening and closing, it may be worthwhile to examine the effect of synchronizing the pulser with the MTS machine to ensure the signal is sent while the crack is closed. It would be interesting, and potentially beneficial, to understand the direct effect the crack face has on the transmission.

## 6. References


1. Mansour, T.M., “Ultrasonic Inspection of Spot Welds in Thin-Gage Steel,” *Materials Evaluation* **46** (1988) 650-658.

2. Newman, John A., “Life Prediction of Spot Welds: A Fatigue Crack Growth Approach,” Master’s Thesis, Virginia Tech, 1997.

3. Rokhlin, S.I., S. Meng, L. Adler, “In-Process Ultrasonic Evaluation of Spot Welds,” *Materials Evaluation* **47** (1989) 935-943.

4. Swellam, M.H., P. Kurath, and F.V. Lawrence, “Electric-Potential-Drop Studies of Fatigue Crack Development in Tensile-Shear Spot Welds,” Advances in Fatigue Lifetime Predictive Techniques, ASTM STP 1122, M.R. Mitchell and R.W. Landgraf, Eds., American Society for Testing and Materials, Philadelphia, pp. 383-401.

5. Vary, A. In *The Acousto-Ultrasonic Approach, Acousto-Ultrasonics: Theory and Applications*, ed. J.C. Duke, Jr. Plenum Press, New York, 1988, pp. 1-21.

6. Aduda, B. and R.D. Rawlings, “Spectral analysis of acousto-ultrasonic waves for defect sizing,” *NDT & E International* **29 (4)** (1996) 237-240.

7. Molina, G. J. and Y. M. Haddad, “Acousto-ultrasonics approach to the characterization of impact properties of a class of engineering materials,” *International Journal of Pressure Vessels and Piping* **67 (3)** (1996) 307-315.

8. Vary, A. “Acousto-Ultrasonic Characterization of Fiber Reinforced Composites,” *Materials Evaluation* **40** (1982) 650-654.

9. Govada, A., E. G. Henneke, R. Talreja, “Acousto-Ultrasonic Measurements to Monitor Damage during Fatigue of Composites,” *1984 Advances in Aerospace Sciences* **8** (1984) 55-60.

10. Mittelman, A., I. Roman, A. Bivas, I. Leichter, J. Marguiles, and A. Weinreb, In *Acousto-Ultrasonic Characterization of Physical Properties of Human Bones, Acousto-Ultrasonics: Theory and Applications*, ed. J.C. Duke, Jr. Plenum Press, New York, 1988, pp. 305-309.

11. Guo, A. and P. Cawley, “Lamb wave propagation in composite laminates and its relationship with acousto-ultrasonics,” *NDT & E International* **26 (2)** (1993) 75-84.

12. Sundaresan, M. J. and E.G. Henneke, II, “Measurement of the Energy Content in Acousto-Ultrasonic Signals,” *Acousto-Ultrasonics: Theory and Applications*, ed. J.C. Duke, Jr. Plenum Press, New York, 1988, pp. 275-282.

13. Sundaresan, M. J. and E.G. Henneke, II, K. L. Reifsnider, and D. Post, “Nondestructive Evaluation of Filament Wound Pressure Vessels, CCMS-87-02,” Center for Composite Materials and Structures, Virginia Tech, 1987.

14. Duke, J. C., “Acousto-Ultrasonics,” *NDE Testing Techniques*, eds. D. F. Bray and D. McBride, Wiley Interscience, NY, 1992.

15. Cooper, J. F. and R. A. Smith, “The Measurement of Fatigue Cracks at Spot-Welds,” *International Journal of Fatigue*, July 1985, pp. 137-140.

16. Overbook, J. L. and J. Draisma, “Fatigue Characteristics of Heavy-Duty Spot-Welded Lap Joints,” *Metal Construction and British Welding Journal*, July 1974, pp. 213-219.

17. McMahon, J. C., G. A. Smith, and F. V. Lawrence, “Fatigue Crack Initiation and Growth in Tensile-Shear Spot Weldments,” *ASTM STP 1058*, H. I. McHenry and J. M. Potter, Eds., American Society for Testing and Materials, Philadelphia, 1990, pp. 47-77.

18. Sperle, J-O, “Strength of spot welds in high strength steel sheets,” *Metal Construction*, April 1983, pp. 200-203.

19. Kan, Yih- Renn, “Fatigue Resistance of Spotwelds – An Analytic Study,” *Metals Engineering Quality*, November 1976, pp.26-36.

20. Karhnak, S. J. and J.C. Duke, Jr., “Predicting Performance of Adhesively Bonded Joints Based on Acousto-Ultrasonic Evaluation,” *Composites Bonding, ASTM STP 1227*, Dennis J. Damico, Thomas L. Wilkinson, Jr., and Sandra L. F. Niks, Eds., American Society for Testing and Materials, Philadelphia, 1994.

21. Cooper, J. F. and R. A. Smith, “Fatigue Crack Propagation at Spot Welds,” *Metal Construction*, Vol. **18**, No. **6**, 1986, pp.383-386.

22. Sundaresan, M. J., E. G. Henneke, II, and W. D. Brosey, “Acousto-Ultrasonic Investigation of Filament Wound Pressure Vessels,” *Materials Evaluation*, Vol. **49**, No. **5**, May 1991, pp. 601-606, 612.

## Appendix A. Micrographs of Sectioned Specimens Showing Crack Presence at the Tip of the Welded Region

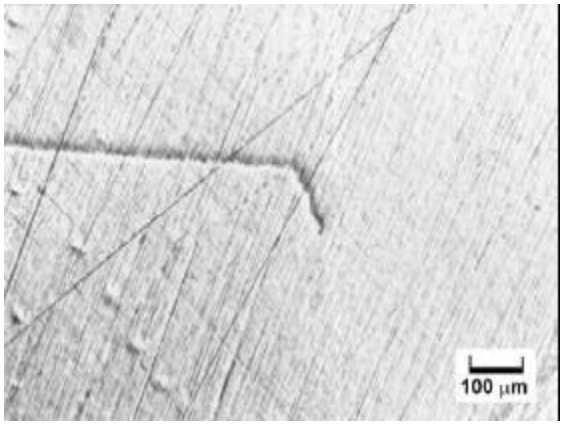


Figure 1. Specimen L1-113

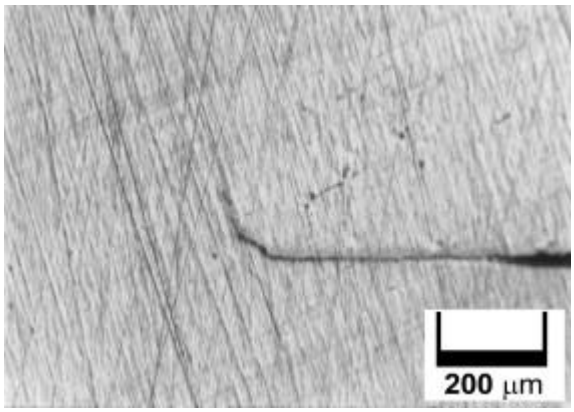


Figure 2. Specimen L1-114

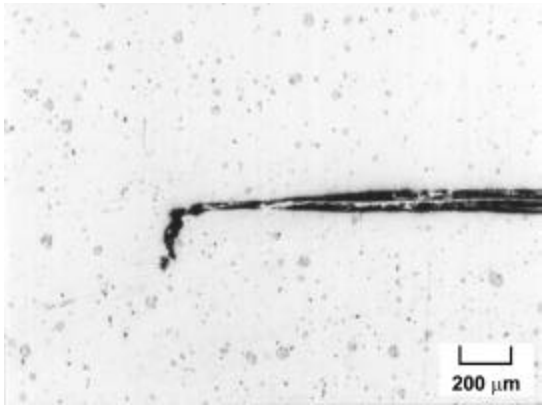


Figure 3. Specimen L1-115

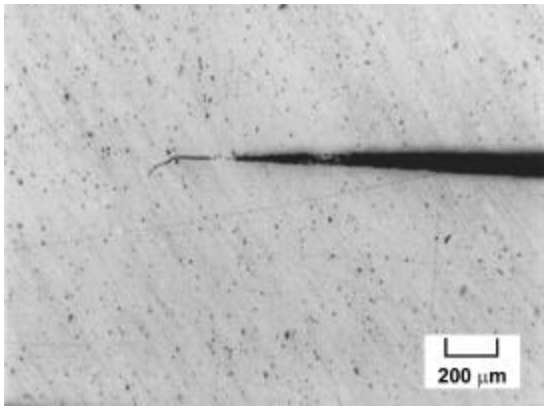


Figure 4. Specimen L1-116

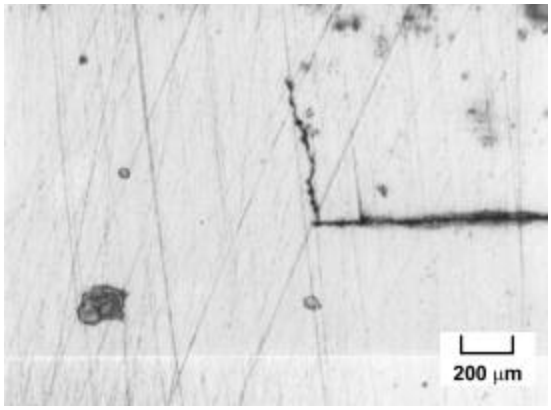


Figure 5. Specimen L1-117

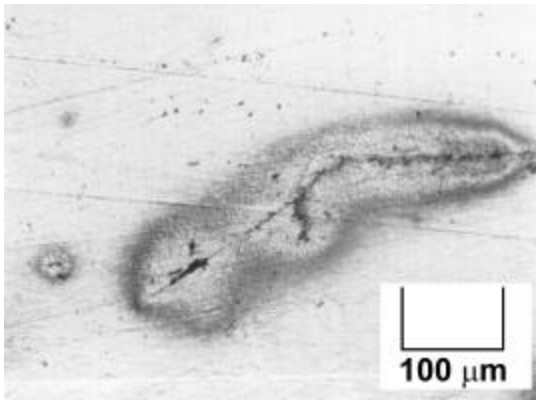


Figure 6. Specimen L1-118

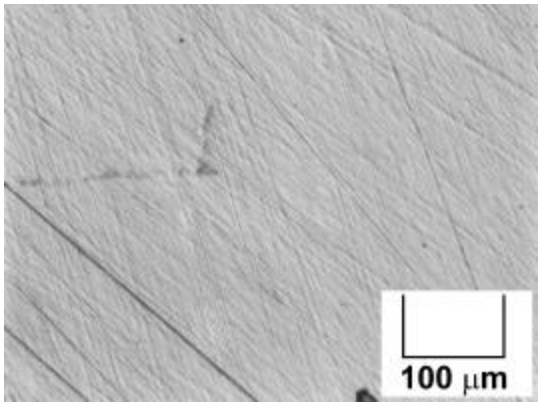


Figure 7. Specimen L1-119

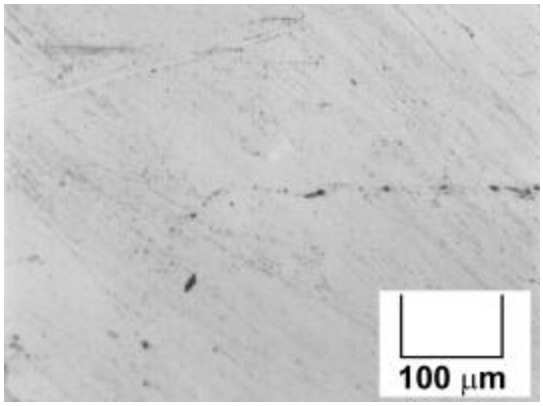


Figure 8. Specimen L1-120

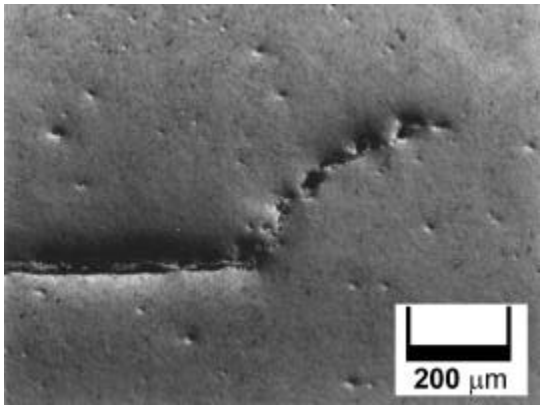


Figure 9. Specimen L1-122

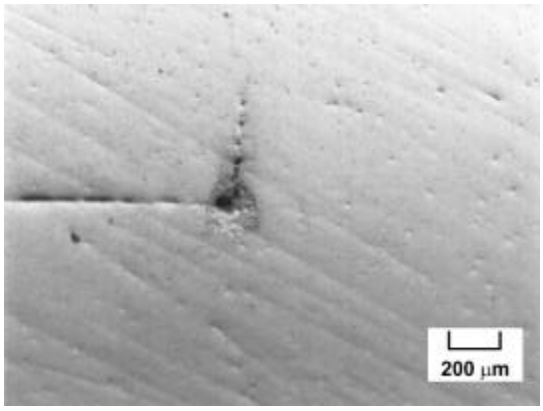


Figure 10. Specimen L1-123

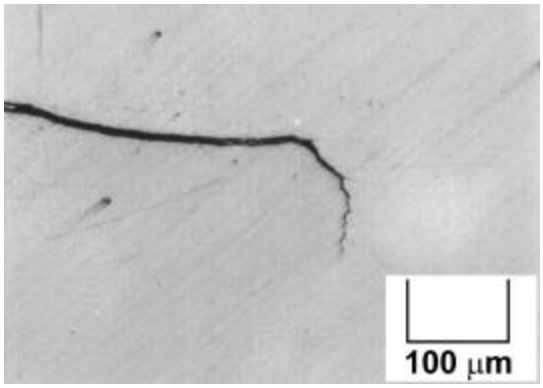


Figure 11. Specimen L9-114

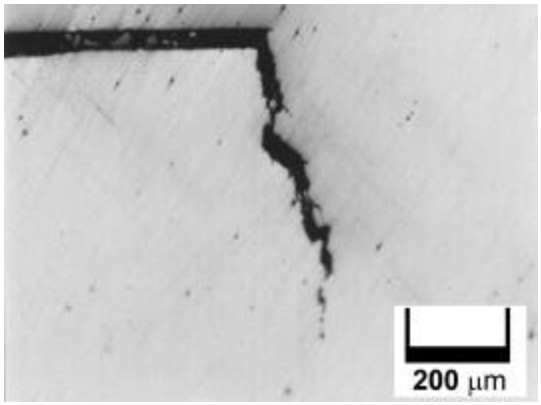


Figure 12. Specimen L9-118

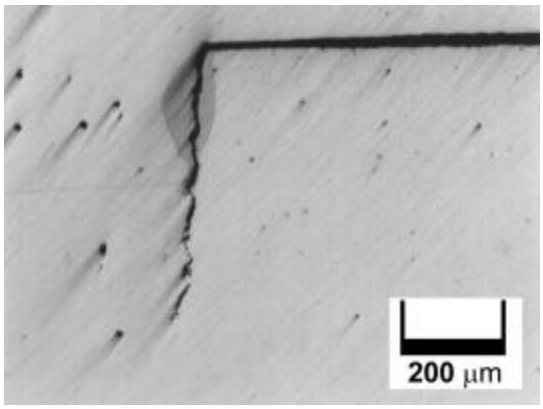


**Figure 13. L9-119**

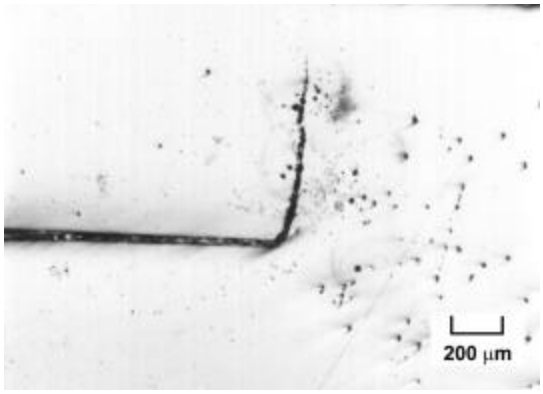


**Figure 14. L9-120**

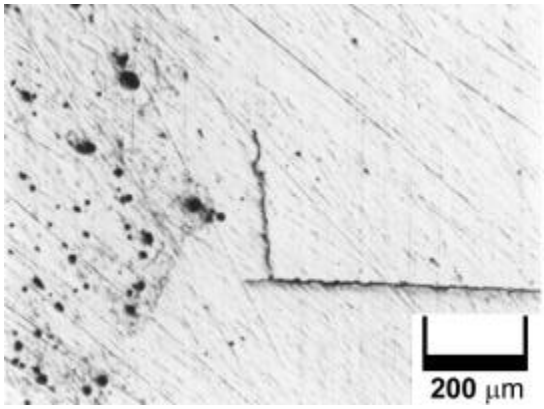


**Figure 15. L9-121**

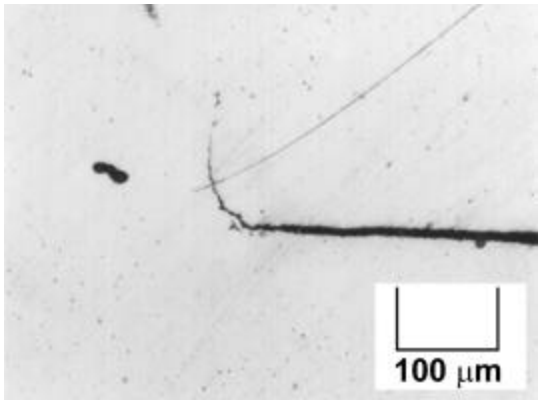


**Figure 16. L9-122**

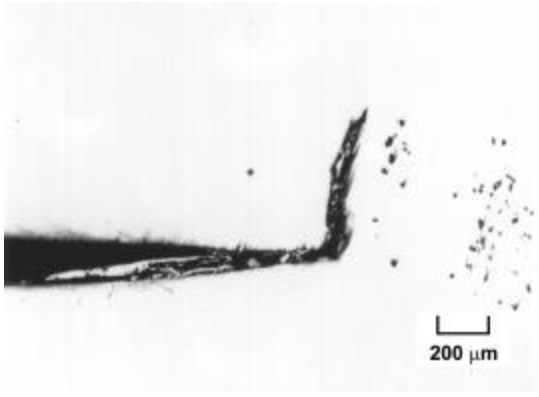


**Figure 17. L9-125**

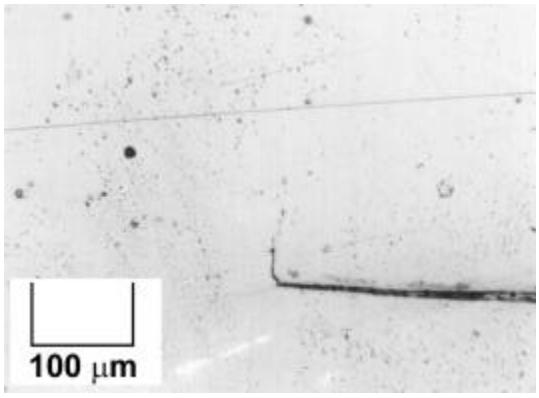


**Figure 18. L9-126**

## VITA

Brian Matthew Gero was born on July 19, 1971 in Asmara, Ethiopia on United States Army Base, Kagnew Station. He moved to the United States approximately 4 months later to Valley Forge, PA where he spent the next year and a half. He then moved to Dale City, VA where he would spend the remaining years of his youth. Brian spent a great deal of time playing soccer growing up, and, during his four years at Gar-Field Senior High School, he was very active on the crew team. He graduated from high school in June of 1989 in the top 5% of his class. He accepted admission into Virginia Tech's engineering department and began his undergraduate program in the fall of 1989. Brian pursued a bachelor's degree in Engineering Science and Mechanics, graduating in May of 1995. He was accepted into the graduate program in Engineering Mechanics where he worked on a FORD sponsored research project under the guidance of Dr. Norman Dowling and Dr. J. C. Duke, Jr.. Brian completed his Master's degree in August of 1997 and is currently pursuing a career in Colorado.